B.P. van der Ploeg

Separating background activity from noise in EMG using a neuromuscular model

TU Delft

Separating background activity from noise in EMG using a neuromuscular model

By

B.P. van der Ploeg

in partial fulfilment of the requirements for the degree of

Master of Science
in Biomedical Engineering

at the Delft University of Technology,
to be defended publicly on Monday October 7, 2019 at 12:45 PM.

Supervisors:	Dr. ir. W. Mugge	TU Delft
	Dr. ir. J.H. de Groot	LUMC
	Ir. K.H. Rodriguez	TU Delft
Thesis committee:	Dr. Ir. A.C. Schouten	TU Delft
	Dr. J.J. van den Dobbelsteen	TU Delft

TU Delft

Contents

Abbreviations

EMG	Electromyography
GL	M. Gastrocnemius Lateralis
GM	M. Gastrocnemius Medialis
SO	M. Soleus
TA	M. Tibialis Anterior
TS	M. Triceps Surae
RMSE	Root Mean Square Error
VAF	Variance Accounted For

Master thesis **2019**

Separating background activity from noise in EMG using a neuromuscular model

Bart van der Ploeg

Karen Rodriguez, Jurriaan de Groot, Winfred Mugge

Department of Biomechanical Engineering, Faculty of Mechanical, Material and Maritime Engineering
Delft University of Technology, 2628 CD Delft, The Netherlands

ABSTRACT

To objectively diagnose the severity of spasticity, it is important to measure the muscle activity accurately. Filtered EMG has an offset above zero which is part noise and part background activity. The goal of this study is to separate these two parts, using a non-linear neuromuscular ankle model. The model uses positional and EMG data as inputs to make a prediction of the output torque around the ankle, optimizing several muscle parameters. It was assumed model error was partly caused by the lack of separation of background activity and noise in the EMG offset. The correlation between model error and the force-length relationship of the muscle was investigated, as it was hypothesized that the force-length relationship could be used to separate background activity from noise in EMG.

Twelve subjects (11 male, 1 female, mean age 25.2±1.7 years) participated in the study, which was approved by the TU Delft Human Research Ethics Committee. The Achilles ankle perturbator and the TMSi Porti7 EMG system were used to obtain positional and EMG data around the ankle. The subjects performed several trials containing multiple ramp-and-hold phases. The trials were performed while relaxed, and while performing co-contraction at 5% and 10% of maximum voluntary co-contraction. Model validity was judged on robustness and fit. Model fit shows how close the predicted torque resembles the measured torque. High robustness is defined as a low variance of the model parameters per subject, between trials. To improve robustness, two model configurations, one using averaged data and one simplified model configuration, were compared with the original model. The most robust model configuration was used as a basis for an alternative model, which added a parameter for each EMG signal, that subtracted part of the EMG offset. This EMG offset subtraction parameter was added to remove the constant part of the noise in the EMG offset. The correlation between model error and the force-length relationship of the model was calculated for the model with the best robustness, and the alternative model.

Model robustness was not improved in the averaged data model configuration or the simplified model configuration, compared to the original model. The original model was therefore used for the rest of the study. The EMG offset subtraction parameter did not yield to desired reduction of noise in the EMG offset. This was likely a result of difficulties with determining the EMG offset. Only weak correlations ($R<<0.3$) were found between the model error and the force-length relationship of the muscles, for both the original model and the alternative model configuration.

1. Introduction

Spasticity is a movement disorder that often occurs after damage of the upper motor neurons. This damage can be present due to stroke, Cerebral Palsy, Multiple Sclerosis, spinal cord injuries or traumatic brain injuries (Adams and Hicks, 2005, Dietz and Sinkjaer, 2007, Sommerfeld et al., 2012). It is estimated that spasticity affects over 12 million people worldwide (Marques et al., 2017). Spasticity is defined as velocity-dependent hyperactivity of the muscle stretch reflex with increased tendon jerks (Lance, 1980). Based on the severity of the spasticity different treatments are available, such as physical therapy, Botulinum Toxin injections or surgery. Current methods to determine the severity of spasticity are qualitative and subjective (Blackburn et al., 2002). To determine the severity of spasticity, it is essential to objectively measure the muscle activity and muscle parameters, to get a good indication of the hyperactivity (Albani et al., 2010).

De Vlugt et al., 2010 proposed a neuromuscular model, with the goal to quantify muscle parameters in stroke patients. The model predicted the generated torque from the ankle rotation and used positional data around the ankle and surface electromyography (EMG) of the M. Tibialis Anterior (TA), M. Soleus (SO), M. Gastrocnemius Medialis (GM) and M. Gastrocnemius Lateralis (GM) as inputs (De Vlugt et al., 2010, Sloot et al., 2015). The predicted torque is calculated by incorporating the passive and active muscle components, as well as inertia and gravity around the ankle joint. The passive component comprises the elastic and relaxation behaviour of the muscles. The active components incorporate the active state, the force-length relationship and the force-velocity relationship of the muscles.

Nevertheless the model still presents limitations. There is an error between the predicted torque and the actual torque to which the model is optimized. Part of the model which is prone to errors, is the EMG, which is used to indentify muscle activation and calculate the active state. In the model, the EMG is filtered with an initial high-pass filter, to remove movement artefacts and low frequent noise. Next the signal is rectified and subsequently low-pass filtered to obtain the envelope and remove high frequencies introduced by rectifying (Sloot et al., 2015).
However, the resulting EMG data typically shows a consistent offset above zero. This can be seen Fig. 1, which shows an example a filtered EMG signal, in which the subject was in rest (blue line) for the first 12 seconds. In the original model this offset is considered noise and is subtracted from the signal (De Vlugt et al., 2010). However this EMG offset contains background activity and not just noise (Burne et al., 2005, Dietz and Sinkjaer, 2007). Therefore complete subtraction of the EMG offset is incorrect and a way of separating the background activity and noise is required. Considering background activity is enhanced in patients with spasticity, who have trouble controlling the activation in their muscles (Burne et al., 2005), it is likely that this subtraction of the offset is a contributor to the model error.

Considering that EMG signals are used to determine the muscle active state, there is an interaction between EMG and other parts of the model, which influence the active component of muscle torque. These two parts are the force-length and the force-velocity relationship of the muscle, which state that the amount of force a muscle can deliver changes depending on its length and velocity (Bobbert et al., 1990, Vandewalle et al., 1987). Considering the EMG offset is most easily identified in rest, the force-velocity relationship is not a useful metric to separate the background activity from noise. However, it has been suggested that the force-length relationship of the muscle can be used to separate background activity from noise in EMG (Sloot et al., 2015). At different muscle lengths in rest, the force-length relationship should be able to be used to identify different levels of background activity. To evaluate if this is true, the model will be used without the subtraction of the EMG offset.

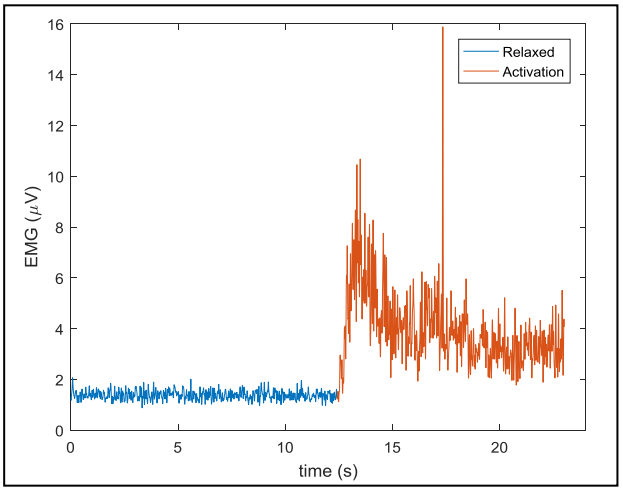

Fig. 1: Example of a filtered EMG signal. Subject was relaxed (blue line) for the first 12 seconds, and then started activating the measured muscle (red line). The EMG while relaxed shows an offset above zero.

In this study it is hypothesized that there is a relationship between the model error and the force-length relationship of the muscle and it is assumed that the model error is for a part a result of incorrect separation between background activity and noise in the EMG offset. If such a relationship is found, this would indicate that the force-length relationship can be used to separate the background activity and noise more accurately. The goal of the study is to further improve the neuromuscular model and estimate the background activity in EMG signals. Improving the model will help with future diagnoses of patients with spasticity, providing a way to determine muscle parameters and activity more accurately and objectively.

1.1 Approach

To test the hypothesis, spasticity was emulated in healthy subjects with a co-contraction task. Co-contraction increases the EMG offset, and increases the relative contribution of background activity in the EMG offset. By performing co-contraction at a higher level, the relationship between the EMG offset and the force-length relationship should become stronger. The trials were also performed while relaxed. The subjects underwent several ramp-and-hold trials, with the holds at different muscle lengths. The different locations of the hold phases provided information about the force-length relationship at different resting lengths of the muscle.

Previous work judged the validity of the model mostly by examining the model fit (De Vlugt et al., 2010, De Gooijer-Van de Groep et al., 2013). The focus of this study was on model robustness, which states how well a model functions when the inputs change. Robustness can be judged by evaluating the variance of the parameters within the subjects, between trials. The subjects performed the trials at different levels of co-contraction, as well as relaxed, which changes the activation input to the model more significantly than in previous studies, where subjects were relaxed throughout all trials (De Vlugt et al., 2010, De Gooijer-Van de Groep et al., 2013, Sloot et al., 2015). To improve model robustness, two different model configurations were examined and compared to the original model configuration. One configuration involved averaging of data over trials, such that the input is more uniform and the effects of outliers are reduced. The other model configuration is a simplified version of the model. With less model parameters to tune, robustness of the other parameters should increase. The model with the best robustness was used as a basis for an alternative model, which included a parameter that removed a constant part of the EMG offset. The alternative model was created with the goal of removing a constant part of the noise in the EMG offset. By removing a constant noise level, the remaining variable noise could be stronger related to the force-length relationship of the muscle. As the parameter subtracts a percentage of the EMG offset, it is expected that this percentage will become lower with higher co-contraction, as the EMG offset is raised with more constant muscle activity. The original model and the alternative model were tested in parallel for the hypothesis that the model error is related to the force-length relationship of the muscle. The model approach is shown in Fig. 2.

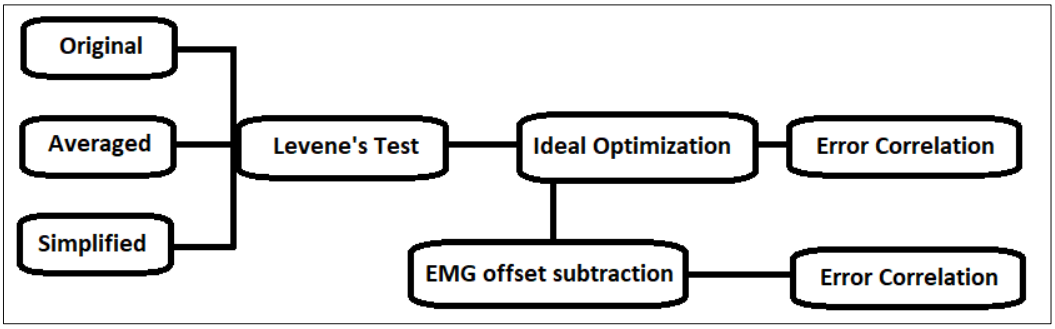

Fig. 2: Model approach. The three different model configurations were compared with the Levene's test. If there was a significant difference between the variances of the optimization methods, the optimization with the lowest variance would be used. If there was no difference between the variances, the original model would be used. The chosen model would be used as a basis for an alternative model with the EMG subtraction parameter added. Both the chosen model and the alternative model were used for the error correlation to test the hypothesis.

2. Methods

2.1 Data collection

2.1.1 Subjects

A total of 12 subjects (11 male, 1 female, mean age 25.2±1.7 years) were recruited to participate in this study. Detailed subject demographics are shown in Table 1. The subjects all gave their written consent. The study was approved by the TU Delft Human Research Ethics Committee.

Table 1 – Subject demographics

Subject	Age	Weight (kg)	Height (cm)	Sex
1	25	74	170	M
2	27	98	205	M
3	26	85	178	M
4	26	100	188	M
5	27	66	183	M
6	23	88	191	M
7	22	62	168	F
8	23	60	173	M
9	26	73	176	M
10	27	72	176	M
11	26	81	188	M
12	24	64	177	M

2.1.2 Instrumentation

The measurements were performed with the Achilles ankle perturbator (MOOG, Nieuw-Vennep), Fig. 3. The Achilles can apply and measure position and torque around the ankle. EMG was measured with the bipolar Porti7 EMG system (TMSi B.V., The Netherlands). Both the EMG and the Achilles sampled at 2048 Hz.

Fig. 3: Achilles ankle perturbator (MOOG, Nieuw-Vennep)

A fault in the Achilles caused it to skip a sample every 430 samples. The missing samples were compensated by interpolation. All data was downsampled to 512 Hz before analysis. The EMG signals were high-pass filtered with a 3rd order recurrent Butterworth filter at 20 Hz. Afterwards the signals were squared, in order to rectify the signals and to increase the relative activation compared to the offset. Lastly the EMG was low-pass filtered with a recurrent Butterworth filter at 20 Hz. The angle and torque data obtained with the Achilles system was low-pass filtered with the same recurrent low-pass Butterworth filter (De Vlugt et al., 2010, Garcia and Viera, 2011).

2.1.3 Participant setup

Before measurements, EMG electrodes were placed on the M. Soleus (SO), M. Gastrocnemius Medialis (GM), M. Gastrocnemius Lateralis (GL) and M. Tibialis Anterior (TA), according to the SENIAM standard (Hermens et al., 2000). The reference electrode was placed on the kneecap.

Next, the ankle angle was placed in the initial position, at 15 degrees plantar flexion, where zero degrees is defined as the anatomical position. This angle was chosen because the tension on the Achilles tendon is

minimal (Davis et al., 1999). The knee angle was positioned at 45 degrees flexion, where a zero angle is defined as complete knee extension. These angles were determined by goniometry.

The passive Range of Motion (ROM) around the ankle was determined in rest, using a torque dependent plantar [Tmax = 10 Nm] and dorsal flexion [Tmax = -15 Nm] protocol (Sloot et al., 2015), in which the ankle was rotated in both directions, until the boundary torques were met.
Next, two step based isometric force tasks were performed, in plantar and dorsal flexion direction, to determine gains for the EMG for each of the muscles, such that activation of each muscle could be compared relative to each other (Schouten et al., 2008). Afterwards the maximum voluntary co-contraction (MVCC) was determined. The subjects were asked to co-contract maximally, while the ankle was in the initial position. Using the obtained gains to compare activation of the muscles relative to each other and the measured torque, it was determined whether co-contraction was performed. The average activation over three maximum co-contraction trials was used to define MVCC.

2.1.4 Measurement trials

The subjects underwent trials which consisted of multiple ramp-and-holds over the whole range of motion around the ankle, see Fig. 4.

To minimize the history-dependent effects of muscle thixotropy (Kusumojati, 2018), each trial started with a pre-conditioning, consisting of five sinusoidal movements at 0.33 Hz, with an amplitude covering 80% of the ROM.
Within 3 seconds after the end of the pre-conditioning, the first ramp was performed. The hold time after each ramp was randomized between 3 and 3.5 seconds. In total, 15 ramp-and-holds were performed in a single trial. The velocities of the ramps were 50, 62.5, 75, 87.5 and 100 degrees per second. Each velocity was repeated 3 times throughout the trial. Between each trial, at least 30 seconds of rest was given.

2.1.5 Passive and active tasks

The trials were performed passively (condition 1), where the subjects were asked to remain relaxed, and actively (conditions 2 and 3), where the subjects were asked to co-contract their ankle muscles. In condition 2 subjects were asked to co-contract at 5% EMG activity of the MVCC and in condition 3 the subjects were asked to co-contract at 10% of the MVCC. Real time EMG was visualized as seen in Fig. 5. A blue line represented the required percentage of the MVCC. A green line represented the real time percentage of the TA muscle activation (the dorsal flexion component of co-contraction). The red line represented the averaged percentage of plantar flexion activation, the GM, GL and the SO muscles, which together make up the M. Triceps Surae (TS).

The subjects trained co-contracting at 10% activation three times before the measurements. If the subjects were not deemed ready the training was repeated. In total 18 trials were performed by each subject, with 6 trials per condition. The order of the trials was randomized.

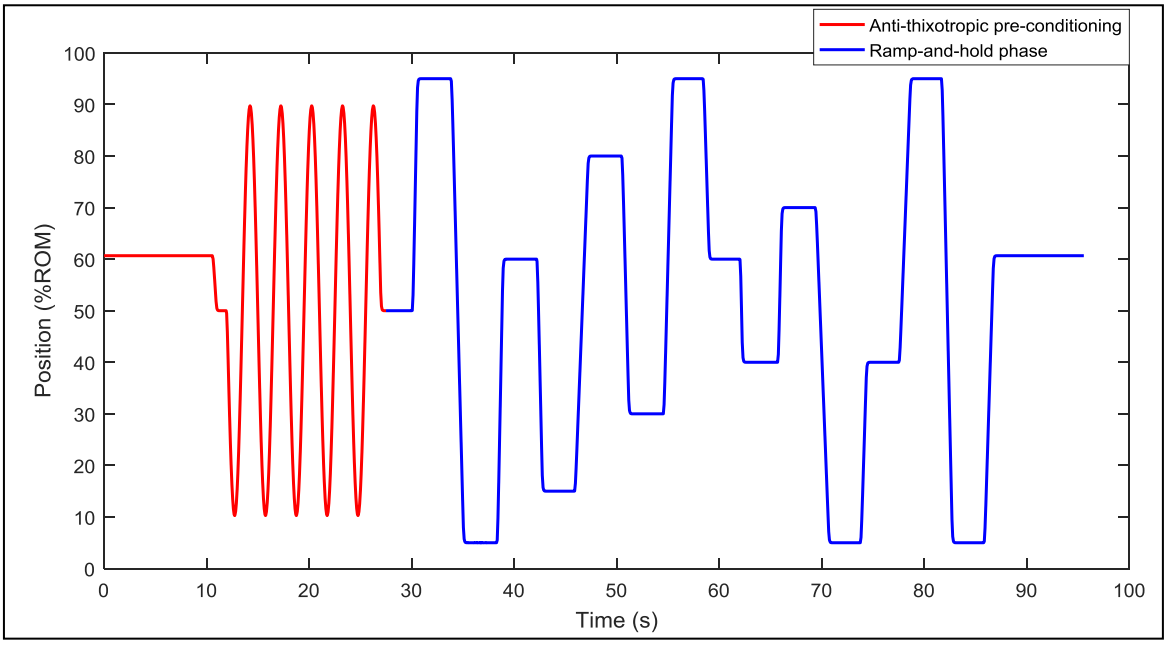

Fig. 4: Applied ankle angle over time during a single trial.

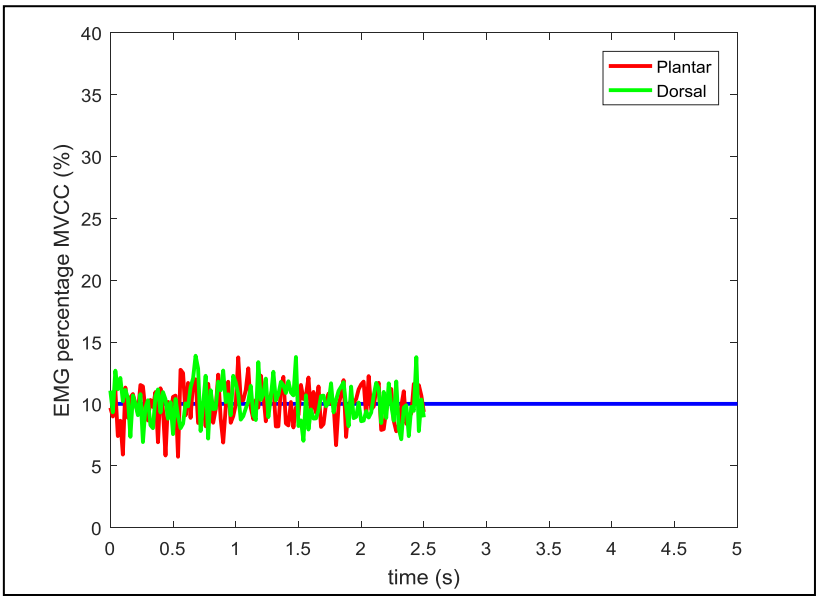

Fig. 5: Representation of the real time EMG on screen. The blue line represents the required EMG level. The green line represents percentage of TA activity. The red line represents the average percentage of activity of the GM, GL and the SO muscles.

2.2 Model optimization

2.2.1 Neuromuscular model

The non-linear neuromuscular model used in this study was first described in De Vlugt et al, 2010. The model incorporates EMG data in combination with positional (ankle rotation) data, to predict the torque around the ankle joint. The predicted torque is calculated by incorporating the passive and active muscle components, as well as the inertia and gravity of the foot around the ankle joint. Several muscle parameters are estimated during the model optimization, shown in Table 2. The model has been further developed over the years (De Vlugt et al., 2012, De Gooijer-Van de Groep et al., 2013, Sloot et al., 2015, Van de Poll 2015). The model used in the present study is based on the model as presented by De Gooijer-Van de Groep et al., 2013. In their version of the model the parallel elastic element includes the exponential force-length and force-velocity functions, while the series elastic element, the tendon, is assumed to be infinitely stiff. The model is fully described in Appendix A.

2.2.2 Optimization

The obtained data was cut such that only the ramp-and-hold phases, and not the anti-thixotropic pre-conditioning, were analysed. A non-linear least squares optimization was used to fit the model parameters. The function tolerance was set to 10^{-6} and the maximum amount of iterations to 15,000. The upper and lower bounds of the parameters are shown in Table 3. The bounds were chosen based on previous work (De Gooijer-Van de Groep, 2019).

Table 2 – Description of the parameters optimized in the model.

Parameter	Description	Unit
m	Mass foot+footplate	kg
k_{tri}	Stiffness coefficient TS	1/m
k_{tib}	Stiffness coefficient TA	1/m
$x_{0,tri}$	Slack length TS	m
$x_{0,tib}$	Slack length TA	m
τ_{rel}	Relaxation time constant	s
k_{rel}	Relaxation factor	-
$g1$	EMG weighting factor for TA	N/V
$g2$	EMG weighting factor for GL	N/V
$g3$	EMG weighting factor for SO	N/V
$g4$	EMG weighting factor for GM	N/V
$l_{0,tri}$	Optimal muscle length TS	m
$l_{0,tib}$	Optimal muscle length TA	m
f_0	Cut-off frequency activation filter	Hz
β	Relative damping coefficient activation filter	-

Table 3 – Starting values and bounds for the optimized parameters.

Parameter	Starting Value	Lower bound	Upper bound
m	1.5	1.2	3
k_{tri}	100	100	600
k_{tib}	100	100	600
$x_{0,tri}$	0.05	0.01	0.09
$x_{0,tib}$	0.05	0.01	0.11
τ_{rel}	2	0.1	6
k_{rel}	0.1	0.05	1
$g1$	1000	1	10^{10}
$g2$	1000	1	10^{10}
$g3$	1000	1	10^{10}
$g4$	1000	1	10^{10}
$l_{0,tri}$	0.048	0.02	0.09
$l_{0,tib}$	0.068	0.02	0.11
f_0	2	0.5	4
β	1	0.5	1.25

2.2.3 Model fit

Previous work judged the model validity by the fit (De Vlugt et al., 2010, De Gooijer-Van de Groep et al., 2013, Sloot et al., 2015). Fit shows how close the predicted torque resembles the measured torque. The fit can be determined with the Variance Accounted For (VAF), or with the Root Mean Square Error (RMSE).

$$VAF = \left(1 - \frac{\Sigma\left(T_{meas}(t) - T_{mod}(t)\right)^2}{\Sigma\left(T_{meas}(t)\right)^2}\right) \cdot 100\% \quad (1)$$

$$RMSE = \sqrt{\left(\frac{\Sigma\left(T_{mod} - T_{meas}\right)^2}{n}\right)} \quad (2)$$

In equations 1 and 2, T_{meas} is the measured torque, T_{mod} is the model torque, and n is the total amount of samples. VAF is used in previous studies (De Vlugt et al., 2010, De Gooijer-Van de Groep et al., 2013, Van de Poll, 2015), and describes the "goodness of fit", where 100% is a perfect fit. The RMSE describes the size of the error, where 0 is a perfect fit. Trials in which the VAF was less than 50%, were considered failed optimizations and were excluded for further analysis.

2.2.4 Robustness

An alternative approach to judge the quality of the optimization is robustness. In this study high robustness is defined as a low variance of the parameters per subject, between trials. Low robustness indicates that the optimization is vulnerable to parameter redundancy. A model suffers from parameter redundancy if it is not possible to determine all parameters accurately, due to interaction between them (Cole and McCrea, 2016).

In an attempt to improve the model robustness, three optimization configurations were examined and compared. First, the original optimization used in previous work (De Vlugt et al., 2010, De Gooijer-Van de Groep et al., 2013).

Second, the optimization is performed with the trials averaged over the conditions per subject. By averaging the data, it was expected that outliers were reduced, resulting in a more robust optimization. To average the data, it was required to adjust the data such that all hold phases had the same length.

Third, the optimization is simplified by reducing the number of parameters (certain parameters were given a fixed value). Because potential redundancies, in this configuration, were decreased, a trade-off between fit and robustness was expected. The chosen fixed parameters were the optimal muscle lengths, $l_{0,tri} = 0.047\ m$ and $l_{0,tib} = 0.073\ m$, (De Gooijer-Van de Groep et al., 2019). The optimal muscle lengths are used in the calculation of the active muscle torque where redundancy was expected, due to the multiplication of the force-length relationship, force-velocity relationship and active state.

It is suggested that the second (averaging the data) and third (simplification of the optimization) configuration of the model, should increase the robustness of the model compared to the original optimization configuration. The Levene's test (Trujilo-Ortiz and Hernandez-Walls, 2003) was used to determine if there was a difference in the variance of the optimized model parameters . The averaged data model configuration and the simplified model configuration were compared with the original model. If a model configuration showed lower variance than the original model on the majority of the parameters, it would be considered more robust. If there was no difference between configurations, the original model would be used.

2.2.5 EMG offset subtraction

With the goal to remove part of the noise in the EMG offset, an alternative model configuration with an added EMG offset subtraction parameter was tested. The minimum EMG was multiplied with a parameter B_x, ranging between 0 and 1, to create a percentage of the offset. This percentage of the offset was subtracted from the total EMG signal.

$$EMG_x = EMG_x - B_x \cdot \min\left(EMG_x\right) \quad (3)$$

Four parameters in the form of B_x were added to the optimization, where x represents the four muscles. The calculation of the minimum EMG is explained in Appendix C. Parameters B_x were evaluated based on the improvement of fit on the total model and its behaviour between conditions.

2.3 Error correlations

The correlation between the error of the model and the force-length relationship of both the TA and the TS was determined with Pearson's correlation coefficient, for each trial. This was done for the model with and without the addition of the parameter B_x. A correlation between 0.3 and 0.5 was considered a moderate correlation and a correlation above 0.5 was considered a strong correlation (Field, 2013). A correlation between 0 and 0.3 was deemed weak and would reject the hypothesis.

3. Results

3.1 Model optimization

Subject ROM is presented in Appendix D. In total 7 trials over all model configurations failed to optimize and were excluded from the evaluation. For more information about the failed optimizations, see Appendix E. Example graphs of the typical measured and estimated torque and EMG for the relaxed and the 10% MCCC activation conditions are shown in Fig. 6. The fit of the original model is shown. The 5% and 10% of MVCC conditions showed similar torque graphs. It is seen that the torque is higher in the co-contraction conditions. In the EMG figure it is seen that the subjects were not able to co-contract constantly throughout the trial, but rather showed an activation pattern related to the movement. It is also seen that the low-pass filter introduces negative overshoot. This negative overshoot is filtered out in the activation filter of the model.

3.1.1 Robustness & fit

Table 4 shows the results of the Levene's test between the original model configuration and the averaged data and the simplified model configuration. The differences in variances between the model configurations is visualized in boxplots in Fig. 7.

Table 4 – Results of the Levene's test. In the case of a significant difference (p<0.05), the model configuration with the smaller variance is named.

Parameter	Original-Averaged	p	Original-Simplified	p
m	Original	0.0000	-	0.6466
k_{tri}	-	0.5740	Original	0.0007
k_{tib}	Averaged	0.0436	-	0.3210
$x_{0,tri}$	-	0.4792	-	0.7200
$x_{0,tib}$	Averaged	0.0018	-	0.9348
τ_{rel}	-	0.9289	-	0.5997
k_{rel}	-	0.1344	-	0.6116
$g_1(TA)$	Original	0.0105	Simplified	0.0002
$g_2(GL)$	Original	0.0000	Simplified	0.0011
$g_3(SO)$	Original	0.0000	-	0.0979
$g_4(GM)$	Original	0.0000	Simplified	0.0000
$l_{0,tri}$	-	0.3101	N/A	N/A
$l_{0,tib}$	Averaged	0.0035	N/A	N/A
f_0	Averaged	0.0095	-	0.4550
β	-	0.1292	-	0.0879

Between the original model configuration and the averaged data model configuration, no difference in variance is found for 6 out of 15 parameters. The original model configuration had a lower variance in 5 parameters and the averaged data model configuration had a lower variance in the remaining 4 parameters.

Between the original model configuration and the simplified model, no difference was found in 9 out of 13 parameters. The original model had a lower variance in 1 parameter and the simplified model had a lower variance in 3 parameters.

The VAF (goodness of fit) and the RMSE (error size) are shown in Table 5. The averaged model configuration had the best fit for both measures, closely followed by the original model. The simplified model showed the worst fit.

Table 5 – Model fit for each of the model configurations, including the model with the EMG offset subtraction parameter, which used the original model as basis.

Fit	Original	Averaged	Simplified	Offset
RMSE	1.5911	1.2546	1.8794	1.7008
VAF	93.3800	94.7876	90.7799	92.4659

Based on these results, it was concluded neither the averaged data model configuration, or the simplified model configuration had a lower variance in the majority of the parameters compared to the original model configuration. Therefore the original model configuration was used to further test the hypothesis.

The mean values for the parameters, in addition to the standard deviation of these parameters, as well as the standard deviation as a percentage of the mean, for each model configuration are shown in Appendix F. An overview of the results per subject is shown in Appendix G.

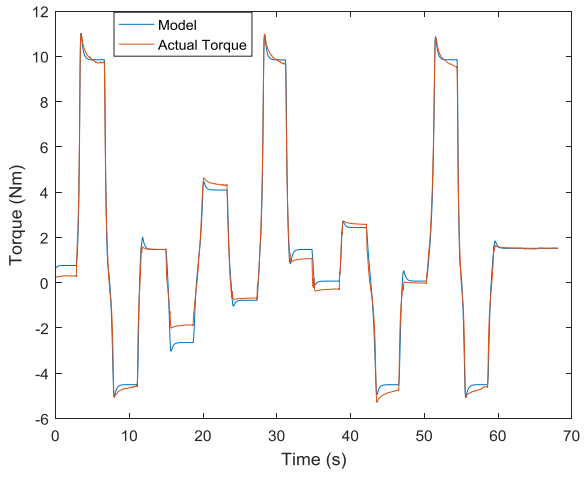

Fig. 6.1: Example of the modeled torque and the measured torque during a relaxed condition trial.

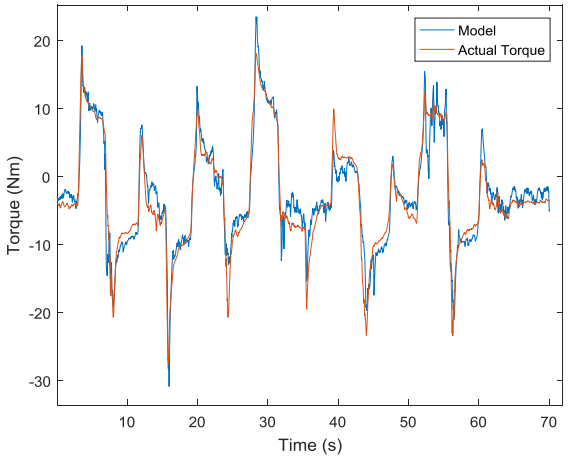

Fig. 6.2: Example of the modeled torque and the measured torque during a 10% MVCC activation trial.

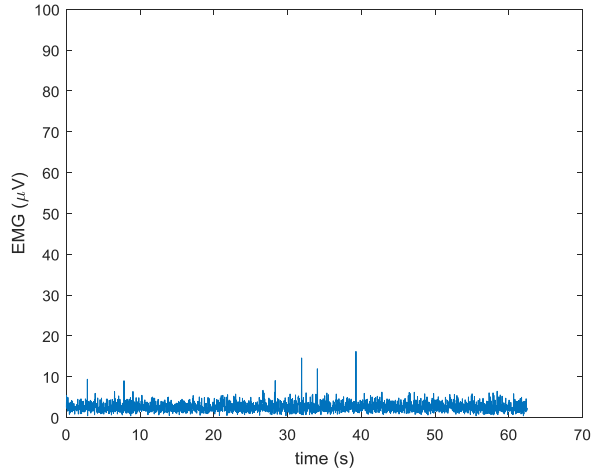

Fig. 6.3: Example of a filtered EMG signal of the GM, during a relaxed condition trial.

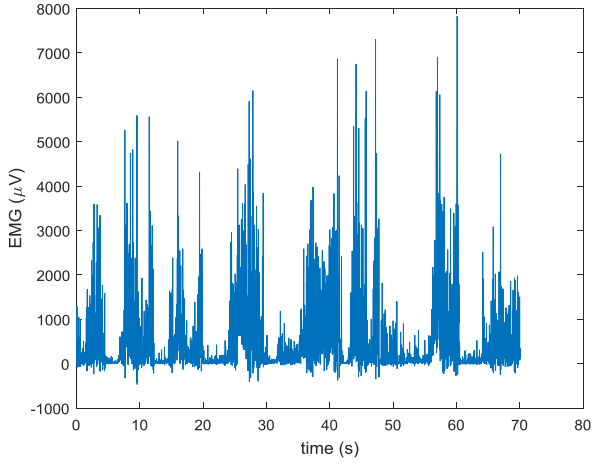

Fig. 6.4: Example of a filtered EMG signal of the GM, during a 10% MVCC activation trial.

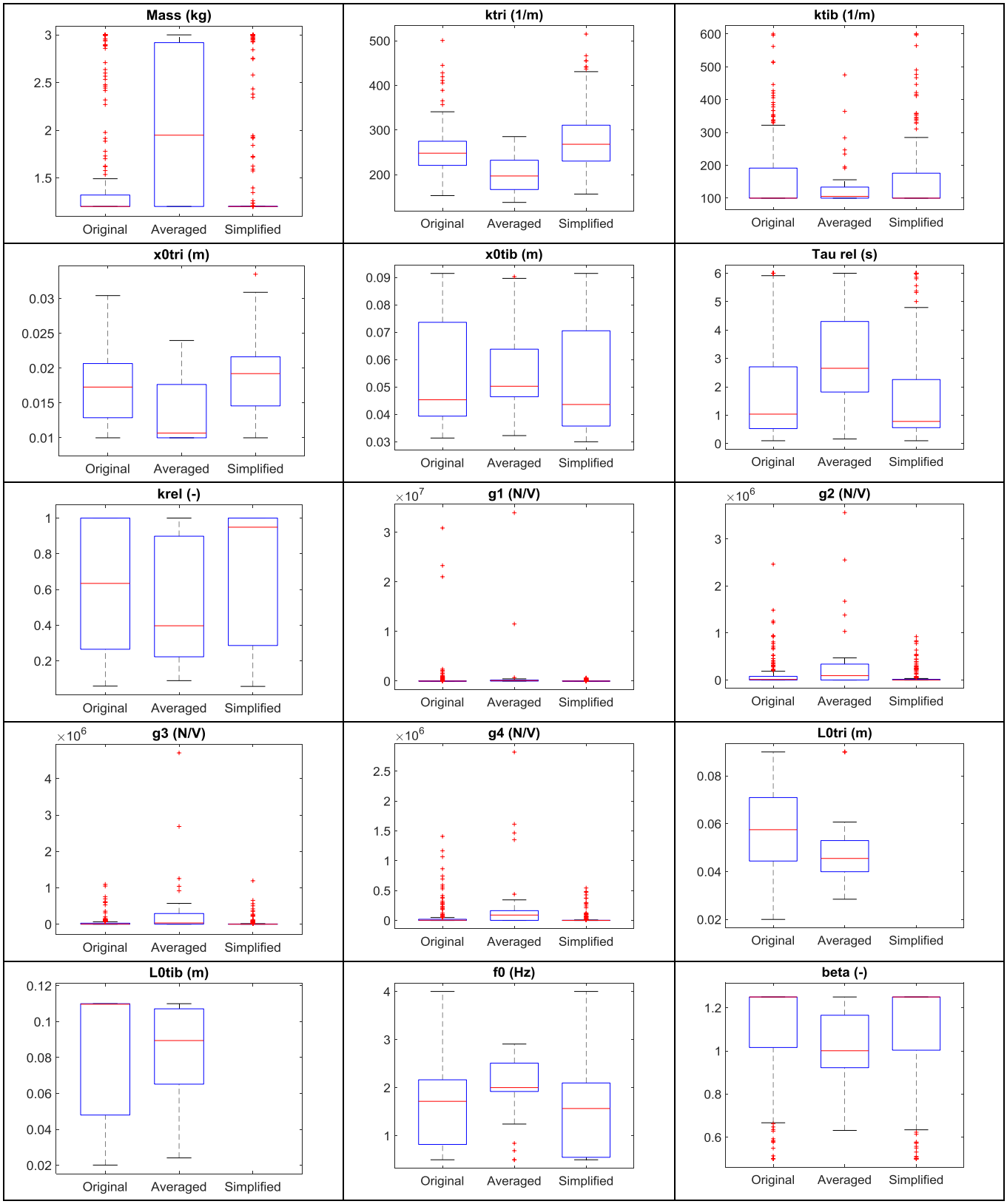

Fig. 7.: Boxplots of all optimized parameters for the original model configuration, the averaged data model configuration and the simplified model configuration.

3.1.2 EMG offset subtraction

Based on the results of the robustness, the original model was used as the basis for the alternative model in which the EMG offset subtraction parameter is added. Table 6 shows the predicted EMG offset subtraction coefficients for each condition. It is seen that the parameter is lower for the rest condition than for the two active conditions. Table 5 shows the model fit. Both the RMSE and the VAF show slightly worse results for the model with the EMG offset subtraction parameter compared to the original model.

An overview of all the optimized parameters for each condition, using the alternative model is shown in Appendix F. The parameters per subject are shown in Appendix G.

3.2 Error correlations

The model error is plotted against the force-length relationship for a typical trial in Fig. 8. Table 7 shows the correlations between the model error and the force-length relationship of the muscles for the original model configuration. Table 8 shows the correlation for the alternative model configuration. Both the force-length relationship of the TA and the TS was evaluated. In the original model, the correlation was significant ($p<0.05$) in 178 of 213 trials for the TS and in 151 of 213 trials for the TA. For the alternative model the correlation was significant in 182 of 213 trials for the TS and in 166 of 213 trials for the TA. The found correlation coefficients indicated a weak ($R<0.3$) correlation for both model configurations in all conditions.

Table 6 – Averaged EMG offset parameter over all trials, and for each condition. Average standard deviation (ASD) of the subjects included.

Parameters	mean	ASD	Rest (C1)	ASD	5% (C2)	ASD	10% (C3)	ASD
$B_1(TA)$	0.1205	0.2130	0.0641	0.1031	0.1547	0.2074	0.1467	0.2437
$B_2(GL)$	0.4772	0.4104	0.2353	0.1509	0.6026	0.3569	0.5971	0.3933
$B_3(SO)$	0.4794	0.4119	0.2373	0.1557	0.5992	0.3578	0.6050	0.4011
$B_4(GM)$	0.4739	0.4080	0.2400	0.1583	0.5894	0.3526	0.5956	0.3949

Table 7 – Average correlation between model error and the force-length relationships of the muscle, for the original model configuration. Shown are the mean Pearson's correlation coefficient R, its standard deviation, the number of trials which showed a significant effect ($p<0.05$) and the mean p-values.

Condition	R ($f_l(x_{tri})$)	SD	p<0.05	Mean p	R ($f_l(x_{tib})$)	SD	p<0.05	Mean p
Total mean	-0.0387	0.1127	178/213	0.0658	-0.0187	0.1718	151/213	0.1223
Rest (C1)	-0.0970	0.1492	65/72	0.0385	-0.0492	0.2730	52/72	0.1021
5% (C2)	-0.0086	0.0819	58/70	0.0793	-0.0133	0.0850	50/70	0.1206
10% (C3)	-0.0093	0.0634	55/71	0.0801	0.0068	0.0707	49/71	0.1445

Table 8 – Average correlation between model error and the force-length relationships of the muscle, for the alternative model configuration. Shown are the mean Pearson's correlation coefficient R, its standard deviation, the number of trials which showed a significant effect ($p<0.05$) and the mean p-values.

Condition	R ($f_l(x_{tri})$)	SD	p<0.05	Mean p	R ($f_l(x_{tib})$)	SD	p<0.05	Mean p
Total mean	-0.0654	0.1598	182/213	0.0584	-0.0377	0.2265	166/213	0.0961
Rest (C1)	-0.1363	0.1817	66/72	0.0321	-0.0925	0.3528	64/72	0.0410
5% (C2)	-0.0157	0.1049	60/70	0.0629	-0.0133	0.0702	50/70	0.1145
10% (C3)	-0.0425	0.1577	56/71	0.0807	-0.0061	0.1398	52/71	0.1339

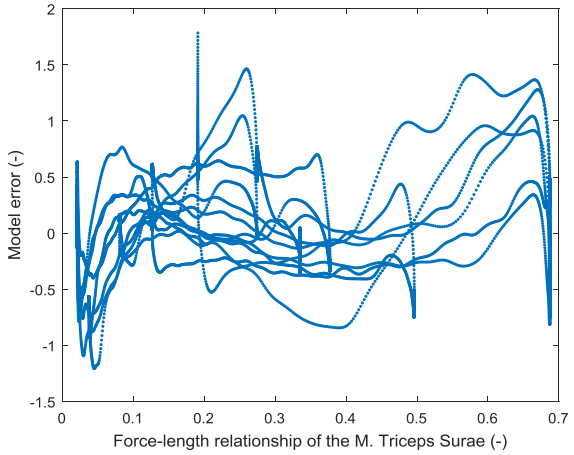

Fig. 8.1: Typical example of the relationship between the model error and the force-length relationship of the TS, for the original model configuration.

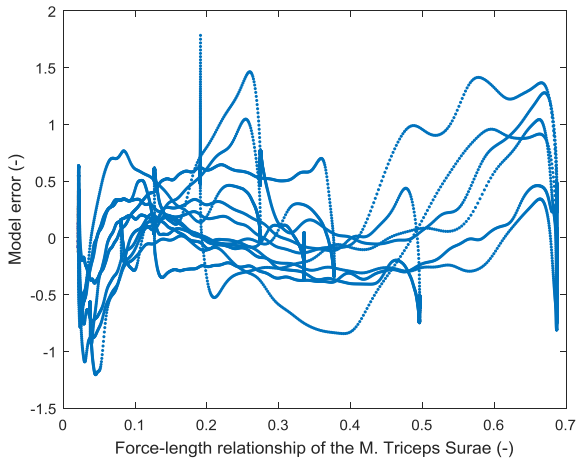

Fig. 8.2: Typical example of the relationship between the model error and the force-length relationship of the TA, for the original model configuration.

4. Discussion

The goal of this study was to improve the neuromuscular model proposed by De Vlugt et al. (2010) and De Gooijer-Van de Groep et al., (2013), by separating the background activity from noise in the EMG offset. It was hypothesized that the model error was correlated to the force-length relationship of the muscle. As it was assumed that the model error was partly a result of the incorrect separation of background activity and noise in the EMG, a correlation would indicate the possibility to separate the background activity and noise. Better separation of background activity and noise would help with objective diagnosing of patients with spasticity. To improve model robustness, two new model configurations were suggested, one using averaged data (over trials per subject) and one simplified (less optimized parameters). These configurations were compared to the original model on robustness, but neither showed lower parameter variance. Next, an alternative optimization of the original model with the addition of an EMG offset subtraction parameter was tested. The EMG offset subtraction parameter was introduced with the goal of removing part of the noise from the EMG offset before correlations were calculated. The new EMG offset subtraction parameter did not improve the model fit. Only very weak correlations ($R<<0.3$) were found between the model error and the force-length relationship for both the original model configuration and the alternative model.

4.1 Robustness & fit

Previous studies judged optimization validity mainly on model fit in the form of the VAF, which describes the goodness of fit (De Vlugt et al., 2010, De Gooijer-Van de Groep et al., 2013, Sloot et al., 2015). While some attention has been given to other forms of model validity, specifically in the original paper by De Vlugt et al., (2010), such as if and how much parameters contribute to the torque, the variance of the parameters within subjects was not discussed. Because the model parameters are all muscle properties that should be independent of the task and input, low variance within subjects is an important metric for model validity. Robustness was especially interesting in the current study because it featured 3 different conditions, in which the subjects were given different tasks, which is in contrast with most previous work, where the subjects were asked to remain relaxed throughout the trials (De Vlugt et al., 2010, De Gooijer-Van de Groep et al., 2013 and Sloot et al., 2015). The different tasks greatly changed the inputs to the model, as activation was much larger. The output torque was also affected by the tasks, as can be seen in Fig. 6.

To examine if model robustness could be improved, two different model configurations, one using averaged data and one simplified version, were compared with the original model configuration. Neither of them showed a lower variance on the majority of the parameters in comparison with the original model configuration. This was surprising, as the averaged data configuration reduced outliers, which was expected to lead to a lower variance in the parameters. For the simplified model configuration, it was expected that parameter redundancy would be reduced as there are less parameters interacting, which should lead to higher robustness. Both alternate model configuration made sacrifices compared to the original model, with the goal to improve robustness. In the averaged data configuration the signals had to be adjusted, such that hold phases were the same length, which meant that information was lost. In the simplified model the optimal muscle lengths were fixed, which meant that these were not accurate for all subjects. In addition simplifying the model lead to an expected reduction of model fit. As the improvement in robustness was not observed, the original model configuration was used for the rest of the study.

Studying the robustness of the original model itself, when observing the standard deviation as a percentage of the mean (Appendix F), the least robust parameters were the EMG weighting factors. This was expected as the EMG is the most noisy input, even after filtering, making the weighting factors difficult to optimize. In addition, the SO, GM and GL are used in the model to create a single activation pattern for the TS. This

could introduce redundancies between the weighting factors of the three muscles. The EMG weighting factors should be especially difficult to optimize in the relaxed condition. As there is little activation, the model could have problems fitting the gains to this low level activation. As a result a larger variance in the EMG gains was expected for the relaxed condition. This is not directly seen in the results, as the variance of the EMG gains is large in all conditions.

Other parameters that showed low robustness (standard deviation more than 50% of the mean), were the stiffness coefficient of the TA, the relaxation time constant and the relaxation factor. These parameters all show large differences in the means between the relaxed condition and the active conditions. This indicates that each of these parameters are incorrectly affected by the activation of the muscles. This could be a result of redundancy between the passive and active muscle torque.

It is interesting that the stiffness coefficient for the TS was one of the most robust parameters, in contrast to the stiffness coefficient of the TA, despite the fact that they are modeled in a very similar manner.

In line with previous work (De Vlugt et al., 2010, De Gooijer-Van de Groep et al., 2013, Sloot et al., 2015), the model fit was good in all conditions (average VAF > 90%), indicating that the model torque closely resembled the actual torque. The relaxed condition (average VAF of 98.5%) showed a better fit than the active conditions (average VAF of 90.9% & 90.4%). This is likely a result of more noisy torque in the active conditions, as seen in Fig. 6, which makes it harder to fit the torque accurately. The size of the error shows a similar pattern, as the RMSE is smaller in the relaxed condition (average RMSE of 0.49) compared to the active conditions (average RMSE of 2.03 & 2.30). The size of the error was more than four times as large in the active conditions, compared to the relaxed condition. Looking at the overall hypothesis of the study, it is likely that the model error in the active conditions, due to its size, is effected more strongly by factors other than the lack of separation of the background activity of the muscle and the noise in the EMG offset.

4.2 EMG offset subtraction

An EMG offset subtraction parameter was introduced into an alternative model configuration, as a way to remove a constant part of the noise in the EMG offset.. An improved fit compared to the original model was expected, because of a reduction in noise, and because there were simply more things to tune within the optimization. In addition it was expected that the parameter would be smaller in higher co-contraction tasks, because co-contraction elevates the EMG offset and therefore the relative amount of background activity compared to noise should be higher. Compared to the original model, the fit was slightly worse over all trials, both in the form of the goodness of fit (VAF) and the size of the model error (RMSE). When separated by condition, the 5% activation condition showed a better fit in the alternative model than the original model. All fits were in a similar range for both model configurations, and the expected meaningful improvement of fit was not observed. This indicates that the EMG offset subtraction parameter was not capable of actually reducing the noise level in the optimization. The parameter values between conditions also did not optimize as expected. The average value of parameter B_x was larger in the active conditions compared to the relaxed condition, for each muscle. This would indicate that the noise is a relative larger part of the EMG offset in co-contraction than while relaxed, which goes against expectations. Lastly it is noted that the parameters for the SO, GM and GL muscles showed very similar values. This is odd as each signal is separate from each other and should feature its own level of noise, and therefore its own optimal level of subtraction. It suggests that there is an amount of redundancy, as these differences might be tuned elsewhere in the model, likely with the EMG weighting factors. The parameter does not seem to have had the desired effect of removing noise from the EMG offset.

A likely cause is the way the EMG offset is calculated. As shown in Fig. 6, the EMG shows negative overshoot as a result of the low-pass filter. This negative overshoot did not affect to rest of the model, as it was filtered out in the activation filter, however it did affect the calculation of the EMG offset, which was done based on the low-pass filtered EMG. Two solutions were considered. The first involved changing the order of the low-pass filter of the EMG to 1. A first order filter has no overshoot, which would make the calculation of the EMG offset easier and more reliable. This option was rejected however, because the model was based on the original model, only with the addition of the offset subtraction parameter. Changing the method of EMG filtering would change the model and make it more difficult to compare with the original model. The second option, which was used in this study, reduces the effect of negative overshoot by using the absolute values of the filtered EMG signal to calculate the offset. While the overshoot still goes below the EMG offset, the effect of the overshoot on the calculation of the offset is strongly reduced. Because the overshoot is present after high peaks, and the offset is calculated over a period of time, it was assumed that the small remaining overshoot had little effect on the calculation of the offset. Based on the results, this might have not been the case.

A second reason why the EMG offset subtraction parameter did not have the desired effect, might be because of problems with co-contraction in the subjects. Subjects deemed proper co-contraction difficult, and as seen in Fig 5., the activation regularly dropped below the desired level. As a result the EMG offset was not actually higher in the co-contraction condition, compared to the relaxed condition. This does not explain why the parameter values are higher than in the relaxed condition, because if there is no difference in offset, the same subtraction would be expected.

If EMG offset subtraction is tested again in the future, priority should be placed on a better way of calculating the EMG offset.

4.3 Error correlations

The results of the correlation were similar between the original model and the alternative model. The absolute correlation coefficients for the alternative model were slightly larger than the original model, but not to the point that the conclusion would be different. Pearson's correlation coefficient between the model error and the force-length relationship of both the TA and the TS was found to be low ($R<<0.3$), indicating a weak correlation. Nonetheless, this correlation was significant ($p<0.05$) in a majority of the trials. This is likely a result of the large amount of data samples ($n>10.000$) used in each correlation. The low correlation coefficients indicate that the force-length relationship of the muscle is likely not affecting the EMG offset. However, due to potential redundancy in the model, it is possible that within the optimization this correction in the offset is compensated by another metric. The passive muscle torque is, for instance, also related to muscle length, as this influences the elastic stiffness. Therefore it might be possible that a missing part of the active muscle torque, a potential relationship between force-length and activation, is incorrectly captured in other parameters. However due to the fact that the correlation was not just very small, but almost non-existent,

other possible explanations for the EMG offset might be of preference for future studies.

4.4 Limitations

The task of co-contraction performed by the subjects was by many deemed very difficult. As a result, the co-contraction activity was not as constant as initially anticipated, as seen in Fig 5. In the extreme positions throughout the movement it was nearly impossible for most subjects to co-contract to the required level. This means the emulation of spasticity was not ideal. Partly this was the result of the used protocol. Because multiple subjects had trouble co-contracting, the MVCC found was likely an underestimation of the actual MVCC. As a result the 5% and 10% of MCCC were also an underestimation, which made it very difficult for the subjects to control activation at this low required level.

Secondly, this study was for a large part based on the assumption that the model error is for a large part a result of the lack of separation of the background activity and noise in the EMG. However with higher activation, the model error increased significantly. This made it likely that other factors started to influence the error more strongly. As a result the hypothesis becomes more difficult to test as the model error is no longer a good representation of the problem of the lack of separation between background activity and noise in the EMG offset.

4.5 Future research

Future research should focus on improving the robustness of the model between active and passive tasks. With more activity, the model fit decreases and several muscle parameters are optimized differently. As all parameters are independent of activation, the model optimization should get similar results in active and passive conditions. Two of the parameters that showed low robustness were the relaxation factor and the relaxation time constant. Both parameters are the only parameters that are a part of the relaxation dynamics of the muscle. This indicates that this part of the model is especially vulnerable to robustness issues. Further model development should therefore focus on improving the relaxation dynamics.

To investigate the EMG offset, a different way of activation should be used during tasks, compared to the co-contraction used in the present study. Co-contraction did not successfully elevate the EMG offset. Research with patients is the ideal option.

Lastly, when using the model to further study the EMG offset, priority should be set to isolating different causes of the model error. If other causes of model error can be separated, the assumption that the model error is related to the EMG offset will become stronger. This will make it easier to use model error to find a way to separate background activity from noise in EMG.

5. Conclusion

In this study a non-linear neuromuscular model was used to find a method of separating background activity from noise in the EMG offset. It was hypothesized that the model error and the force-length relationship of the muscles were correlated, assuming that the model error was partly a result of the lack of separation between the noise and background activity in the offset of the EMG signals. Model robustness was attempted to be improved by comparing the original model configuration with a model configuration using averaged data and a simplified model configuration. An alternative model configuration was developed containing an EMG offset subtraction parameter, with the goal of removing a constant part of the noise in the EMG offset. Model robustness was not improved in the averaged data model configuration or the simplified model configuration, compared to the original model. Model fit was found to be good for the original model (VAF>90%, RMSE<1.6). The EMG offset subtraction parameter did not yield the desired reduction of noise in the EMG offset. Only weak correlations (R<<0.3) were found between the model error and the force-length relationship of the muscles, for both the original model and the alternative model with the EMG offset subtraction parameter.

6. References

Adams, M. M., & Hicks, A. L. (2005). Spasticity after spinal cord injury. *Spinal cord*, *43*(10), 577-586.

Albani, G., BE, S. V., Bar, D., Campanelli, L., BE, R. G., & Mauro, A. (2010). Use of surface EMG for evaluation of upper limb spasticity during botulinum toxin therapy in stroke patients. *Functional neurology*, *25*(2), 103.

Blackburn, M., van Vliet, P., & Mockett, S. P. (2002). Reliability of measurements obtained with the modified Ashworth scale in the lower extremities of people with stroke. *Physical therapy*, *82*(1), 25-34.

Bobbert, M. F., Ettema, G. C., & Huijing, P. A. (1990). The force-length relationship of a muscle-tendon complex: experimental results and model calculations. *European journal of applied physiology and occupational physiology*, *61*(3-4), 323-329.

Burne, J. A., Carleton, V. L., & O'dwyer, N. J. (2005). The spasticity paradox: movement disorder or disorder of resting limbs?. *Journal of Neurology, Neurosurgery & Psychiatry*, *76*(1), 47-54.

Cole, D. J., & McCrea, R. S. (2016). Parameter redundancy in discrete state-space and integrated models. *Biometrical Journal*, *58*(5), 1071-1090.

Davis Jr, W. L., Singerman, R., Labropoulos, P. A., & Victoroff, B. (1999). Effect of ankle and knee position on tension in the Achilles tendon. *Foot & ankle international*, *20*(2), 126-131.

De Gooijer-Van de Groep-Van de Groep, K. L., De Vlugt, E., De Groot, J. H., Van der Heijden-Maessen, H. C., Wielheesen, D. H., Van Wijlen-Hempel, R. M. S., Arendzen, J. H., & Meskers, C. G. (2013). Differentiation between non-neural and neural contributors to ankle joint stiffness in cerebral palsy. *Journal of neuroengineering and rehabilitation*, *10*(1), 81.

De Gooijer-Van de Groep-Van de Groep, K.L. (2019). *Identification of neural and non-neural contributors to joint stiffness in upper motor neuron disease* (Doctoral dissertation). http://hdl.handle.net/1887/74470

De Jong, M. (2015). The design of a new protocol to acccurately estimate the passive and active components of the muscle system. http://resolver.tudelft.nl/uuid:aff7c662-24cb-4ec2-92a5-0ce69902c947

De Vlugt, E., De Groot, J. H., Schenkeveld, K. E., Arendzen, J., Van

der Helm, F. C., & Meskers, C. G. (2010). The relation between neuromechanical parameters and Ashworth score in stroke patients. *Journal of neuroengineering and rehabilitation*, *7*(1), 35.

Dietz, V., & Sinkjaer, T. (2007). Spastic movement disorder: impaired reflex function and altered muscle mechanics. *The Lancet Neurology*, *6*(8), 725-733.

Field, A.P. (2013). *Discovering statistics using IBM SPSS statistics*. (4th ed.). London: Sage.

Garcia, M. C., & Vieira, T. M. M. (2011). Surface electromyography: Why, when and how to use it. *Revista andaluza de medicina del deporte*, *4*(1), 17-28.

Hermens, H. J., Freriks, B., Disselhorst-Klug, C., & Rau, G. (2000). Development of recommendations for SEMG sensors and sensor placement procedures. *Journal of electromyography and Kinesiology*, *10*(5), 361-374.

Kusumojati, A. (2018). Resting period induces time and mechanical-history dependence in muscle thixotropy around the human ankle joint. http://resolver.tudelft.nl/uuid:582da96a-bbbe-4716-b81b-9039450758a6

Lance, J. W. (1980). Pathophysiology of spasticity and clinical experience with baclofen. In R. G. Feldman, R. R. Young, & W. P. Koella (Eds.), *Spasticity: Disordered motor control*. Chicago: Yearbook Medical.

Maganaris, C. N., Baltzopoulos, V., & Sargeant, A. J. (1998). In vivo measurements of the triceps surae complex architecture in man: implications for muscle function. *The Journal of physiology*, *512*(2), 603-614.

Maganaris, C. N., & Baltzopoulos, V. (1999). Predictability of in vivo changes in pennation angle of human tibialis anterior muscle from rest to maximum isometric dorsiflexion. *European Journal of Applied Physiology and Occupational Physiology*, *79*(3), 294-297.

Marques, I. A., Silva, M. B., Silva, A. N., Luiz, L. M. D., Soares, A. B., & Naves, E. L. M. (2017). Measurement of post-stroke spasticity based on tonic stretch reflex threshold: implications of stretch velocity for clinical practice. *Disability and Rehabilitation*, 1-7.

Schouten, A. C., De Vlugt, E., & Van Der Helm, F. C. (2008). Design of perturbation signals for the estimation of proprioceptive reflexes. *IEEE Transactions on Biomedical Engineering*, *55*(5), 1612-1619.

Sloot, L. H., van der Krogt, M. M., van Eesbeek, S., de Groot, J., Buizer, A. I., Meskers, C., ... & Harlaar, J. (2015). The validity and reliability of modelled neural and tissue properties of the ankle muscles in children with cerebral palsy. *Gait & posture*, *42*(1), 7-15.

Sommerfeld, D. K., Gripenstedt, U., & Welmer, A. K. (2012). Spasticity after stroke: an overview of prevalence, test instruments, and treatments. *American journal of physical medicine & rehabilitation*, *91*(9), 814-820.

Trujillo-Ortiz, A. and R. Hernandez-Walls. (2003). Levenetest: Levene's test for homogeneity of variances. A MATLAB file. [WWW document]. URL http://www.mathworks.com/matlabcentral/fileexchange/loadFile.do?objectId=3375&objectType=FILE

Van de Poll, K. D. (2015). Estimating ankle muscle parameters. http://resolver.tudelft.nl/uuid:aac95ba2-f7f2-4a13-818a-890a42f971e5

Vandewalle, H., Peres, G., Heller, J., Panel, J., & Monod, H. (1987). Force-velocity relationship and maximal power on a cycle ergometer. *European journal of applied physiology and occupational physiology*, *56*(6), 650-656.

Appendix A: Neuromuscular model

A non-linear neuromuscular model, first described by De Vlugt et al, 2010, was used in this study. The model has been developed further over the years (De Gooijer-Van de Groep-Van de Groep et al., 2013, Sloot et al., 2015). The model used in the present study is based on the model by De Gooijer-Van de Groep and colleagues from 2013 as well as the model by Van de Poll (2015). The clear presentation by Van de Poll (2015) and De Jong (2015) was used as the source for the code used in the present study. The model makes a prediction of the output torque around the ankle. The total ankle joint torque in the model is described by equation 4:

$$T_{mod}(t) = T_{Inertia}(t) + T_{tri}(t) - T_{tib}(t) + T_{grav}(\theta) \quad (4)$$

In the model a positive torque direction is defined as plantar flexion, while a positive angle direction is described as dorsal flexion. In the model t represents the time [s], and θ the ankle angle [rad]. T_{mod} [Nm] is the output torque predicted by the model. $T_{Inertia}$ [Nm] is the torque provided by the inertia of the foot in combination with the foot plate. The torque generated in plantar flexion direction, by the TS is represented by T_{tri} [Nm]. T_{tib} [Nm] represents the torque generated by the TA, in dorsal flexion direction. Lastly T_{grav} [Nm] represents the torque as a result of gravity.

A.1 Inertial torque

The inertial torque $T_{Inertia}$ is described with equation 5.

$$T_{Inertia}(t) = I \cdot \ddot{\theta} \quad (5)$$

Here $\ddot{\theta}$ is the angular acceleration of the foot. Inertia of the foot plus footplate I is modelled as a point mass and can be described with the following equation:

$$I = m \cdot l_a \quad (6)$$

In this equation m is the combined mass of the foot and footplate, while l_a is the moment arm from the modelled point mass to the centre of rotation around the ankle. In the model l_a is set at 0.10 meters.

A.2 Gravitational torque

The gravitational torque $T_{grav}(\theta)$, uses the same modelled point mass as the previously described inertial torque. A modification has been made compared to the original model. For a further explanation about this modification, see Appendix B.

$$T_{grav}(\theta) = m \cdot g \cdot l_a \cdot \cos\left(\theta + \theta_{fg} - \sin\left(\frac{l_b}{l_a}\right)\right) \quad (7)$$

In this equation g represents the gravitational acceleration ($g = 9.81\ m/s^2$), while θ_{fg} is the angle of the foot compared to the ground at the zero ankle angle in radians. The moment arm is once again described with l_a, and the component from that moment arm, from the point of rotation perpendicular to the footplate, is described with l_b, which is set to 0.09 m in the optimization.

The muscle torques $T_{tri}(t)$ and $T_{tib}(t)$ consist of an elastic (passive) and active component.

$$T_{tri}(t) = (F_{elas,tri} + F_{act,tri}) \cdot r_{tri} \quad (8)$$

$$T_{tib}(t) = (F_{elas,tib} + F_{act,tib}) \cdot r_{tib} \quad (9)$$

Due to the rotation of the foot the moment arms r_{tri} and r_{tib}, at which these torques act vary and are dependent on the ankle angle (Maganaris et al.,1998, Maganaris & Baltzopoulos, 1999).

$$r_{tri} = 0.0480 - 0.0104 \cdot \theta \quad (10)$$

$$r_{tib} = 0.0393 + 0.0171 \cdot \theta \quad (11)$$

These ankle angles can in turn be used to determine the muscle lengths.

$$x_{tri} = l_{m,tri} - 1.67 \cdot r_{tri}(\theta) \quad (12)$$

$$x_{tib} = l_{m,tib} - 1.56 \cdot r_{tib}(\theta) \quad (13)$$

Here $l_{m,tri}$ [m] is the length of the muscle when the ankle is under a 0 radian angle. These muscle lengths are set to $l_{m,tri} = 0.118$ and $l_{m,tib} = 0.136$ [m] (Maganaris, 1998).

A.3 Passive muscle torque

The elastic muscle forces $F_{elas,tri}$ and $F_{elas,tib}$ are dependent on muscle relaxation and passive muscle properties. Initial elastic muscle force can be determined as follows:

$$F_{elas,0,tri}(x_{tri}) = e^{k_{tri} \cdot (x_{tri} - x_{tri,0})} \quad (14)$$

$$F_{elas,0,tib}(x_{tri}) = e^{k_{tib} \cdot (x_{tib} - x_{tib,0})} \quad (15)$$

Here x_{tri} [m] is the aforementioned muscle length, $x_{tri,0}$ [m] is the muscle slack length and k_{tri} [1/m] is the stiffness coefficient. Because the elastic force decreases as a result of relaxation, initial elastic force is affected by relaxation dynamics.

$$F_{elas,tri} = \frac{\tau_{rel} \cdot s + 1}{\tau_{rel} \cdot s + 1 + k_{rel}} F_{elas,0,tri} \quad (16)$$

$$F_{elas,tib} = \frac{\tau_{rel} \cdot s + 1}{\tau_{rel} \cdot s + 1 + k_{rel}} F_{elas,0,tib} \quad (17)$$

In these transfer functions τ_{rel} is the relaxation time constant [s] and k_{rel} is the relaxation factor [-]. Because of the elastic properties of the muscle, it is only possible for F_{elas} to be positive. This means if F_{elas} has a negative value, this value will be set to 0.

$$if\ F_{elas,tri} < 0 \rightarrow F_{elas,tri} = 0 \quad (18)$$

$$if\ F_{elas,tib} < 0 \rightarrow F_{elas,tib} = 0 \quad (19)$$

A.4 Active muscle torque

The active muscle force F_{act} is a product of the muscle active state, the force-length relationship of the muscle and the force-velocity relationship of the muscle.

$$F_{act,tri} = f_l(x_{tri}) \cdot f_v(\dot{x_{tri}}) \cdot a_{tri} \quad (20)$$

$$F_{act,tib} = f_l(x_{tib}) \cdot f_v(\dot{x_{tib}}) \cdot a_{tib} \quad (21)$$

Before the muscle active state a can be obtained, the neural activation E [V] must be obtained from the EMG signals, and the SO, GM and GL signals need to be combined into one measure for activation of the TS.

$$E_{tib}(t) = g_1 \cdot e_1(t) \quad (22)$$

$$E_{tri}(t) = g_2 \cdot e_2(t) + g_3 \cdot e_3(t) + g_4 \cdot e_4(t) \quad (23)$$

Here e_{1-4} represent the four filtered EMG signals of the TA, GL, SO and GM [V]. The gains g_{1-4} [-] are used as weighting factors for the EMG.

Next, the neural activation is subjected to a linear second order filter which describes the muscle activation process.

$$a_{tri} = \frac{\omega_0^2}{s^2 + 2 \cdot \beta \cdot \omega_0 \cdot s + \omega_0^2} \cdot E_{tri}(s) \quad (24)$$

$$a_{tib} = \frac{\omega_0^2}{s^2 + 2 \cdot \beta \cdot \omega_0 \cdot s + \omega_0^2} \cdot E_{tib}(s) \quad (25)$$

In this activation filter $\omega_0 = 2\pi \cdot f_0$, where f_0 describes the cut-off frequency of the filter and β the relative damping.

The force-length relationship of the model describes the overlap of the myosin and actin filaments in the sarcomere, and affects how much force can be generated at different muscle lengths.

$$f_l(x_{tri}) = e^{-\frac{(x_{tri} - l_{0,tri})^2}{wfl_{tri}}} \quad (26)$$

$$f_l(x_{tib}) = e^{-\frac{(x_{tib} - l_{0,tib})^2}{wfl_{tib}}} \quad (27)$$

Here the muscle length [m] is described with x_{tri}, which is explained above. The optimal muscle length [m] is represented with $l_{0,tri}$. The value of wfl_{tri} can be found with the formula $wfl_{tri} = cf \cdot l_{0,tri}$. In this formula $cf = 0.1$ [-], which is a shaping factor for the force length-relationship.

The force-velocity relationship describes how much force can be generated when the muscle is shortening or lengthening at a certain velocity. Because the muscle behaves differently when lengthening or shortening, there is a different formula for when the velocity is positive or negative.

$\dot{x}_{tri} < 0$:

$$f_v(\dot{x}_{tri}) = -\frac{\dot{x}_{tri}+v_{max,tri}}{\frac{\dot{x}_{tri}}{m_{vsh}}-v_{max,tri}} \quad (28)$$

$\dot{x}_{tri} \geq 0$:

$$f_v(\dot{x}_{tri}) = 1 + \frac{(1+m_{vsh}\cdot m_{vshl})(f_{ecc}-1)\dot{x}_{tri}}{m_{vsh}\cdot m_{vshl}\cdot v_{max,tri}+\dot{x}_{tri}} \quad (29)$$

$\dot{x}_{tib} < 0$:

$$f_v(\dot{x}_{tib}) = -\frac{\dot{x}_{tib}+v_{max,tib}}{\frac{\dot{x}_{tib}}{m_{vsh}}-v_{max,tib}} \quad (30)$$

$\dot{x}_{tib} \geq 0$:

$$f_v(\dot{x}_{tib}) = 1 + \frac{(1+m_{vsh}\cdot m_{vshl})(f_{ecc}-1)\dot{x}_{tib}}{m_{vsh}\cdot m_{vshl}\cdot v_{max,tri}+\dot{x}_{tib}} \quad (31)$$

These equations are slightly different from the way they are presented in Van de Poll (2015) and De Jong (2015). The currently presented equations are a correction on a mistake in the presentation of the force-velocity relationship equations in these theses. In the equations $m_{vsh} = 0.25$ [-] and $m_{vshl} = 0.5$ [-] are shaping factors. The maximum eccentric force [N] is represented by f_{ecc}. The maximum eccentric force is 1.5 times the maximum isometric force, which is normalized to 1, meaning $f_{ecc} = 1.5$. Lastly v_{max} [m/s] is the maximum shortening velocity, equal to eight times the optimal muscle length per second. This means that $v_{max,tri} = 8 \cdot l_{0,tri}$.

All parameters that are optimized in the model are shown in Table 2, and are the parameters without a value presented above.

Appendix B: Gravitational torque

In the theses by Van de Poll (2015) and De Jong (2015) the gravitational torque was described as follows:

$$T_{grav}(\theta) = m \cdot g \cdot l_a \cdot \cos(\theta - \theta_{fg}) \quad (32)$$

In this equation θ is the ankle angle in radians and θ_{fg} is the angle of the foot compared to the ground at the neutral ankle angle in radians.

In the model $\theta - \theta_{fg}$ is seemingly assumed to be the angle under which the moment arm of the gravity acts. However this is not correct. Neither the angle of the footplate, nor the angle of the moment arm are described with this statement.
The correct description of the angle of the footplate would be $\theta + \theta_{fg}$. This can be visualized by imagining the ankle in the neutral position, meaning $\theta = 0$. In this situation the plate is under angle θ_{fg}, according to its definition. Therefore to get the angle of the plate at all times, θ_{fg} needs to be added, not subtracted from the ankle angle.

To get the required angle of the momentarm a further manipulation of this statement needs to be performed, which is visualized in Fig. 9. The required angle is angle x. Angle a is the angle of the footplate and is therefore equal to $\theta + \theta_{fg}$. Angle b is known, as $b = pi - a = p - (\theta + \theta_{fg})$. Angle c is also known, if the perpendicular distance from the point of rotation to the plate (lb) is known. Angle $c = \text{asin}(lb/la)$. With the knowledge of angles b and c it is possible to determine the desired angle x:

$$x = pi - b - c = pi - \left(pi - (\theta + \theta_{fg})\right) - asin\left(\frac{lb}{la}\right) = \theta + \theta_{fg} - asin\left(\frac{lb}{la}\right) \quad (33)$$

Now that angle x is known, the correct formula for the gravitational torque can be determined.

$$T_{grav}(\theta) = m \cdot g \cdot l_a \cdot \cos\left(\theta + \theta_{fg} - asin\left(\frac{lb}{la}\right)\right) \quad (7)$$

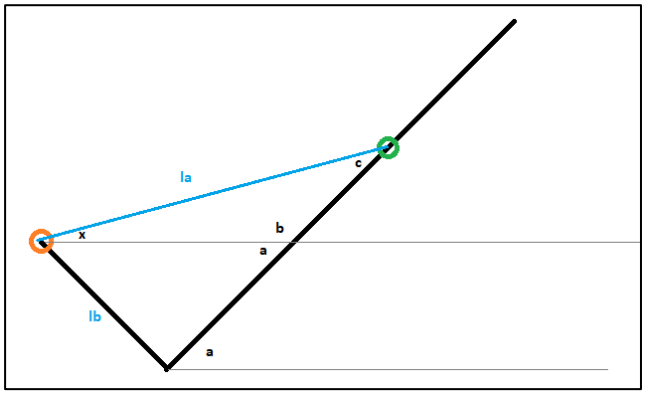

Fig. 9: Visualization of the correct angle under which the gravitational torque functions.

Appendix C: EMG offset subtraction

The low-pass filter of the EMG introduced negative overshoot after high peaks in the EMG signal, as seen in Fig. 6. Because the overshoot was regularly lower than the offset itself, the minimum value of the EMG is no longer representative of the offset. To find the offset, the EMG signals were first divided into segments of 64 samples, 1/8th of the 512 Hz sample frequency. Using the lowest average segment to determine the EMG offset reduced the effects of short overshoot peaks. In addition these segments were taken over the absolute value of the EMG, to further reduce the impact of the negative overshoot peaks.

Appendix D: Subject ROM

Table 9 – ROM data for the subjects. ROM is the total range of motion. ROMmin is the maximum plantar flexion angle and ROMmax is the maximum dorsal flexion angle. A zero angle is defined as the neutral position.

Subject	ROM (°)	ROMmin (°)	ROMmax (°)
1	79.7074	-67.3744	12.33295
2	73.8072	-67.3328	6.474401
3	61.3319	-56.5163	4.815573
4	67.4209	-47.1838	20.23708
5	88.1569	-67.0742	21.08265
6	71.0715	-53.7367	17.33476
7	78.3599	-65.926	12.43385
8	88.4905	-70.4838	18.00667
9	90.2930	-71.4581	18.83493
10	86.8539	-65.0066	21.84726
11	69.7297	-59.7358	9.993851
12	99.7842	-75.3233	24.46092

Appendix E: Failed optimizations

An optimization of a trial was considered failed if the VAF was less than 50 %. These trials were excluded from further analysis, because the model error is so large, that it would be impossible to trace it back to EMG offset. Table 10 shows per optimization configuration how may trials failed to optimize.

Table 10 – Amount of trials that failed to optimize for each model configuration. Total number of failed trials and number of failed trials per condition are presented.

Model configuration	Total	Rest(C1)	5%(C2)	10%(C3)
Original	3	0	2	1
Averaged data	0	0	0	0
Simplified	1	0	1	0
EMG offset parameter	3	0	2	1

Appendix F: Results per condition

Tables 11-14 show the model parameters of the optimization per condition for the original model configuration (Table 11), the averaged data model configuration (Table 12), the simplified model configuration (Table 13) and the alternative model configuration containing the EMG offset subtraction parameters (Table 14). The standard deviation given is the averaged standard deviation over the subjects. This was preferred over the standard deviation over the whole data set, as it gives insight in the variance within the subjects, which is more interesting than the variance between the subjects. The averaged standard deviation is also given as a percentage of the mean, which allows for robustness analyses.

Table 11 – Mean parameter values, model fit and standard deviations after optimization with the original model configuration. Parameters averaged over all trials, as well as averaged per condition are presented. The standard deviations presented are the averaged standard deviation (ASD) over the subjects. The averaged standard deviation as a percentage of the mean is also provided.

Parameter	Total	ASD	ASD%	Relaxed (C1)	ASD	5% (C2)	ASD	10% (C3)	ASD
m	1.472	0.412	28.008	1.546	0.426	1.432	0.246	1.439	0.246
k_{tri}	247.530	51.071	20.632	239.027	33.736	246.772	48.788	256.790	47.437
k_{tib}	158.488	84.322	53.204	225.954	80.370	132.541	28.628	116.969	19.055
$x_{0,tri}$	0.017	0.004	25.429	0.018	0.003	0.016	0.004	0.016	0.004
$x_{0,tib}$	0.053	0.017	32.436	0.072	0.010	0.045	0.007	0.043	0.005
τ_{rel}	1.817	1.684	92.711	2.338	1.310	1.408	1.059	1.704	1.564
k_{rel}	0.623	0.337	54.056	0.317	0.157	0.766	0.221	0.786	0.187
$g_1(TA)$	4.681E+05	1.383E+06	295.459	6.235E+05	1.109E+06	1.412E+04	3.183E+04	7.668E+05	1.204E+06
$g_2(GL)$	1.107E+05	2.316E+05	209.195	2.708E+05	3.382E+05	3.202E+04	4.491E+04	2.922E+04	3.211E+04
$g_3(SO)$	5.193E+04	1.066E+05	205.276	1.148E+05	1.512E+05	2.662E+04	3.759E+04	1.433E+04	1.391E+04
$g_4(GM)$	6.179E+04	1.337E+05	216.331	1.471E+05	1.701E+05	2.199E+04	4.322E+04	1.628E+04	2.139E+04
$l_{0,tri}$	0.058	0.019	31.759	0.053	0.012	0.060	0.018	0.063	0.016
$l_{0,tib}$	0.083	0.031	38.053	0.072	0.026	0.086	0.033	0.090	0.023
f_0	1.593	0.754	47.344	0.964	0.494	1.942	0.596	1.873	0.423
β	1.095	0.216	19.735	1.171	0.110	1.021	0.219	1.094	0.160
RMSE	1.591	0.955	-	0.491	0.344	2.035	0.406	2.300	0.463
VAF	93.380	5.376	-	98.506	2.162	90.945	3.828	90.402	3.740

Table 12 – Mean parameter values, model fit and standard deviations after optimization with the averaged data model configuration. Parameters averaged over all trials, as well as averaged per condition are presented. The standard deviations presented are the averaged standard deviation (ASD) over the subjects. The averaged standard deviation as a percentage of the mean is also provided.

Parameter	Total	ASD	ASD%	Relaxed (C1)	ASD	5% (C2)	ASD	10% (C3)	ASD
m	2.047	0.642	31.35734	2.353	N/A	1.826	N/A	1.960	N/A
k_{tri}	201.980	34.704	17.18189	182.656	N/A	216.492	N/A	206.793	N/A
k_{tib}	142.255	51.825	36.43101	144.591	N/A	169.884	N/A	112.289	N/A
$x_{0,tri}$	0.013	0.003	22.15961	0.013	N/A	0.014	N/A	0.013	N/A
$x_{0,tib}$	0.055	0.012	21.736	0.058	N/A	0.060	N/A	0.048	N/A
τ_{rel}	2.965	1.239	41.79904	2.776	N/A	3.247	N/A	2.872	N/A
k_{rel}	0.505	0.312	61.66143	0.212	N/A	0.669	N/A	0.636	N/A
$g_1(TA)$	1.40E+06	1.52E+06	108.64	1.54E+05	N/A	2.98E+06	N/A	1.05E+06	N/A
$g_2(GL)$	3.85E+05	4.06E+05	105.3442	2.41E+05	N/A	4.94E+05	N/A	4.21E+05	N/A
$g_3(SO)$	3.73E+05	4.44E+05	119.0437	3.52E+05	N/A	5.30E+05	N/A	2.37E+05	N/A
$g_4(GM)$	2.82E+05	3.26E+05	115.9164	2.59E+05	N/A	2.58E+05	N/A	3.28E+05	N/A
$l_{0,tri}$	0.049	0.011	21.87465	0.044	N/A	0.048	N/A	0.054	N/A
$l_{0,tib}$	0.083	0.020	24.25384	0.072	N/A	0.098	N/A	0.079	N/A
f_0	2.029	0.528	26.02464	1.571	N/A	2.317	N/A	2.199	N/A
β	1.010	0.159	15.75333	1.078	N/A	0.996	N/A	0.957	N/A
RMSE	1.255	0.680	-	1.248	N/A	0.935	N/A	1.581	N/A
VAF	94.788	5.256	-	92.694	N/A	98.026	N/A	93.643	N/A

Table 13 – Mean parameter values, model fit and standard deviations after optimization with the simplified model configuration. Parameters averaged over all trials, as well as averaged per condition are presented. The standard deviations presented are the averaged standard deviation (ASD) over the subjects. The averaged standard deviation as a percentage of the mean is also provided.

Parameter	Total	ASD	ASD%	Relaxed (C1)	ASD	5% (C2)	ASD	10% (C3)	ASD
m	1.458	0.293	20.08695	1.602	0.389	1.395	0.064	1.377	0.107
k_{tri}	273.717	58.867	21.50667	238.598	36.209	285.648	41.242	296.906	54.021
k_{tib}	155.617	57.757	37.11461	197.323	52.345	140.755	13.317	128.774	12.816
$x_{0,tri}$	0.018	0.004	22.02974	0.018	0.003	0.019	0.003	0.019	0.003
$x_{0,tib}$	0.051	0.016	30.30467	0.069	0.009	0.044	0.003	0.041	0.004
τ_{rel}	1.663	1.510	90.79355	2.561	1.626	1.185	0.811	1.243	0.893
k_{rel}	0.687	0.324	47.23236	0.348	0.179	0.871	0.129	0.841	0.160
$g_1(TA)$	3.68E+04	7.67E+04	208.2607	1.09E+05	9.11E+04	8.03E+02	6.41E+02	5.84E+02	4.26E+02
$g_2(GL)$	5.86E+04	1.25E+05	213.1433	1.64E+05	1.78E+05	7.32E+03	6.05E+03	4.26E+03	3.32E+03
$g_3(SO)$	3.28E+04	8.15E+04	248.2562	8.92E+04	1.23E+05	6.66E+03	6.40E+03	2.69E+03	2.34E+03
$g_4(GM)$	2.64E+04	6.18E+04	233.8998	7.38E+04	9.14E+04	3.04E+03	4.65E+03	2.50E+03	2.75E+03
f_0	1.582	0.814	51.42518	1.017	0.702	1.994	0.560	1.736	0.531
β	1.093	0.205	18.7432	1.142	0.137	1.052	0.184	1.086	0.199
RMSE	1.879	1.080	-	0.562	0.357	2.347	0.268	2.736	0.348
VAF	90.780	6.685	-	98.079	2.514	87.832	2.988	86.401	3.003

Table 14 – Mean parameter values, model fit and standard deviations after optimization with the alternative model configuration containing the EMG offset subtraction parameter. Parameters averaged over all trials, as well as averaged per condition are presented. The standard deviations presented are the averaged standard deviation (ASD) over the subjects. The averaged standard deviation as a percentage of the mean is also provided.

Parameter	Total	ASD	ASD%	Relaxed (C1)	ASD	5% (C2)	ASD	10% (C3)	ASD
m	1.561	0.448	28.7252	1.714	0.583	1.470	0.177	1.497	0.264
k_{tri}	247.771	54.903	22.15868	228.049	40.724	251.274	36.934	264.358	62.043
k_{tib}	153.407	80.119	52.22663	208.746	87.686	134.983	25.576	115.060	17.405
$x_{0,tri}$	0.017	0.004	25.54311	0.017	0.004	0.017	0.003	0.017	0.004
$x_{0,tib}$	0.053	0.016	29.78243	0.069	0.013	0.046	0.005	0.044	0.004
τ_{rel}	1.874	1.570	83.76752	2.220	1.051	1.660	1.209	1.695	1.544
k_{rel}	0.587	0.341	58.08723	0.264	0.131	0.743	0.209	0.768	0.207
$g_1(TA)$	2.84E+05	9.52E+05	335.2503	6.43E+05	1.22E+06	5.70E+03	9.02E+03	1.93E+05	4.70E+05
$g_2(GL)$	1.08E+05	2.25E+05	207.4068	2.48E+05	3.32E+05	4.68E+04	5.20E+04	2.47E+04	2.95E+04
$g_3(SO)$	4.73E+04	1.08E+05	228.666	8.13E+04	1.08E+05	4.43E+04	7.50E+04	1.41E+04	1.36E+04
$g_4(GM)$	5.86E+04	1.27E+05	216.7372	1.31E+05	1.61E+05	2.53E+04	4.69E+04	1.67E+04	2.43E+04
$l_{0,tri}$	0.059	0.016	27.70573	0.052	0.011	0.062	0.015	0.062	0.014
$l_{0,tib}$	0.082	0.030	37.17988	0.072	0.024	0.086	0.031	0.087	0.027
f_0	1.663	0.722	43.4206	1.217	0.690	1.925	0.480	1.862	0.419
β	1.114	0.195	17.49433	1.162	0.130	1.086	0.183	1.095	0.148
$B_1(TA)$	0.120	0.213	176.7626	0.064	0.103	0.155	0.207	0.147	0.244
$B_2(GL)$	0.477	0.410	85.99567	0.235	0.151	0.603	0.357	0.597	0.393
$B_3(SO)$	0.479	0.412	85.91616	0.237	0.156	0.599	0.358	0.605	0.401
$B_4(GM)$	0.474	0.408	86.0953	0.240	0.158	0.589	0.353	0.596	0.395
RMSE	1.701	1.040	-	0.628	0.511	2.006	0.354	2.513	0.699
VAF	92.466	6.639	-	97.456	3.708	91.415	3.159	88.298	6.580

Appendix G: Results per subject

Tables 15-18 show the model parameters of the optimization per subject for the original model configuration (Table 15), the averaged data model configuration (Table 16), the simplified model configuration (Table 17) and the alternative model configuration containing the EMG offset subtraction parameters (Table 18).

Table 15.1 – Mean parameter values, model fit and standard deviations after optimization with the original model configuration for each subject, over all trials.

Parameter	Subject 1	SD	Subject 2	SD	Subject 3	SD	Subject 4	SD	Subject 5	SD	Subject 6	SD
m	1.531	0.651	1.345	0.305	1.618	0.674	2.788	0.550	1.346	0.425	1.572	0.583
k_{tri}	213.577	22.344	251.929	32.130	255.354	46.360	198.877	27.679	244.205	29.295	230.079	51.644
k_{tib}	131.297	50.605	191.495	104.826	130.488	117.301	347.530	161.824	120.870	39.016	134.717	68.423
$x_{0,tri}$	0.013	0.003	0.015	0.003	0.014	0.004	0.013	0.005	0.017	0.003	0.015	0.005
$x_{0,tib}$	0.051	0.017	0.065	0.018	0.044	0.013	0.077	0.011	0.049	0.014	0.048	0.017
τ_{rel}	2.419	1.294	1.743	1.770	2.664	2.140	1.509	1.113	1.875	1.639	1.339	0.686
k_{rel}	0.749	0.348	0.673	0.329	0.592	0.308	0.331	0.247	0.549	0.335	0.736	0.386
$g_1(TA)$	2.00E+03	4.32E+03	6.64E+04	2.75E+05	2.28E+05	6.11E+05	3.19E+06	8.79E+06	1.25E+03	5.32E+02	2.88E+05	6.89E+05
$g_2(GL)$	1.55E+05	3.31E+05	1.35E+05	2.65E+05	1.94E+05	5.73E+05	4.92E+04	1.02E+05	1.17E+04	1.22E+04	4.67E+04	7.28E+04
$g_3(SO)$	1.54E+04	2.87E+04	8.08E+04	1.90E+05	1.32E+05	3.42E+05	6.85E+04	1.08E+05	5.45E+04	4.50E+04	1.43E+04	2.71E+04
$g_4(GM)$	4.68E+03	6.77E+03	6.25E+04	2.05E+05	1.62E+04	2.45E+04	1.71E+04	6.92E+04	9.56E+03	1.55E+04	2.53E+04	4.46E+04
$l_{0,tri}$	0.059	0.017	0.044	0.016	0.057	0.021	0.049	0.014	0.081	0.016	0.054	0.018
$l_{0,tib}$	0.095	0.028	0.067	0.042	0.079	0.037	0.072	0.030	0.110	0.000	0.082	0.023
f_0	1.574	0.571	1.221	0.571	1.755	0.731	1.465	0.784	2.240	0.481	1.351	0.654
β	1.136	0.158	0.947	0.257	1.213	0.093	1.093	0.200	1.158	0.191	1.216	0.081
RMSE	1.826	0.981	0.931	0.497	2.006	0.973	1.550	0.938	1.847	0.936	2.495	1.714
VAF	91.837	5.673	97.674	1.678	92.918	4.807	96.601	2.632	93.004	4.020	88.141	9.615

Table 15.2 – Mean parameter values, model fit and standard deviations after optimization with the original model configuration for each subject, over all trials.

Parameter	Subject 7	SD	Subject 8	SD	Subject 9	SD	Subj. 10	SD	Subj. 11	SD	Subj. 12	SD
m	1.244	0.129	1.280	0.338	1.205	0.021	1.105	0.433	1.499	0.556	1.133	0.283
k_{tri}	282.176	37.148	276.714	65.707	255.925	65.140	225.224	100.103	259.412	44.224	276.885	91.081
k_{tib}	156.868	76.831	153.800	103.976	142.461	72.669	139.164	97.299	154.119	93.406	99.046	25.682
$x_{0,tri}$	0.020	0.003	0.020	0.005	0.018	0.004	0.017	0.008	0.018	0.003	0.022	0.006
$x_{0,tib}$	0.052	0.021	0.054	0.019	0.050	0.020	0.047	0.026	0.056	0.017	0.044	0.013
τ_{rel}	1.471	1.936	1.457	1.320	1.833	2.316	1.423	1.773	2.708	2.073	1.361	2.152
k_{rel}	0.620	0.340	0.670	0.364	0.781	0.277	0.527	0.376	0.747	0.336	0.501	0.394
$g_1(TA)$	1.18E+04	3.80E+04	1.52E+05	2.91E+05	1.24E+06	4.94E+06	1.68E+05	3.00E+05	1.20E+05	3.57E+05	1.44E+05	2.96E+05
$g_2(GL)$	1.01E+05	2.99E+05	1.43E+05	1.64E+05	1.53E+05	3.78E+05	2.08E+05	3.16E+05	8.69E+04	2.21E+05	4.42E+04	4.40E+04
$g_3(SO)$	4.67E+04	6.01E+04	6.96E+04	1.75E+05	6.90E+03	8.35E+03	1.03E+05	2.37E+05	2.23E+04	3.98E+04	9.22E+03	1.79E+04
$g_4(GM)$	3.62E+04	8.81E+04	1.55E+05	2.20E+05	1.23E+05	3.44E+05	1.70E+05	3.57E+05	1.16E+05	2.23E+05	5.63E+03	7.24E+03
$l_{0,tri}$	0.064	0.014	0.057	0.026	0.065	0.012	0.057	0.024	0.051	0.021	0.064	0.023
$l_{0,tib}$	0.091	0.030	0.092	0.033	0.081	0.040	0.082	0.042	0.058	0.032	0.081	0.040
f_0	1.382	0.606	1.699	0.968	1.820	1.028	1.397	1.040	1.273	0.690	1.942	0.929
β	1.004	0.217	1.073	0.270	1.202	0.098	1.027	0.395	1.063	0.268	1.013	0.365
RMSE	1.179	0.625	1.319	0.742	1.359	0.754	2.081	1.706	0.752	0.338	1.749	1.259
VAF	95.953	2.795	89.903	8.360	94.523	4.582	91.362	10.641	96.312	2.437	92.332	7.266

Table 16.1 – Mean parameter values, model fit and standard deviations after optimization with the averaged data model configuration for each subject, over all trials.

Parameter	Subject 1	SD	Subject 2	SD	Subject 3	SD	Subject 4	SD	Subject 5	SD	Subject 6	SD
m	1.777	0.999	1.892	0.951	1.796	1.032	2.999	0.001	2.850	0.260	2.319	0.625
k_{tri}	210.368	23.865	237.589	67.708	209.210	51.323	184.541	12.359	169.750	6.024	198.802	2.864
k_{tib}	131.693	54.894	252.879	129.501	105.024	8.697	182.935	56.182	101.335	2.311	118.671	32.340
$x_{0,tri}$	0.013	0.004	0.016	0.006	0.011	0.001	0.011	0.002	0.010	0.000	0.011	0.002
$x_{0,tib}$	0.055	0.018	0.076	0.019	0.044	0.011	0.062	0.011	0.053	0.005	0.049	0.015
τ_{rel}	5.237	0.698	3.130	0.510	1.464	1.395	1.781	1.406	2.417	0.123	1.546	0.467
k_{rel}	0.784	0.305	0.423	0.115	0.537	0.402	0.504	0.360	0.419	0.469	0.724	0.478
$g_1(TA)$	1.25E+05	3.10E+04	1.74E+05	2.50E+05	2.78E+04	4.64E+04	1.54E+07	1.69E+07	1.97E+05	1.73E+05	1.65E+05	1.27E+05
$g_2(GL)$	5.99E+05	6.79E+05	3.82E+05	5.68E+05	1.22E+05	1.96E+05	5.29E+04	4.42E+04	2.04E+06	1.84E+06	1.01E+05	1.63E+05
$g_3(SO)$	1.55E+04	1.42E+04	1.01E+06	1.46E+06	2.59E+04	2.24E+04	7.85E+05	4.07E+05	1.92E+06	2.47E+06	3.62E+04	5.08E+04
$g_4(GM)$	6.08E+05	8.70E+05	4.58E+05	7.73E+05	2.83E+04	4.84E+04	2.18E+04	3.77E+04	1.44E+06	1.40E+06	1.25E+05	1.15E+05
$l_{0,tri}$	0.046	0.009	0.042	0.010	0.056	0.029	0.046	0.016	0.076	0.023	0.039	0.009
$l_{0,tib}$	0.101	0.015	0.079	0.037	0.058	0.040	0.049	0.014	0.109	0.002	0.084	0.009
f_0	1.973	0.994	1.502	0.868	1.764	1.001	1.557	0.402	2.550	0.459	2.200	0.365
β	1.092	0.160	0.989	0.268	1.099	0.108	1.220	0.052	1.033	0.124	1.023	0.226
RMSE	0.786	0.402	1.605	2.090	2.346	1.186	0.750	0.295	1.342	0.148	1.398	0.917
VAF	98.557	1.024	89.653	17.031	88.051	12.032	99.229	0.330	96.365	1.771	95.984	3.107

Table 16.2 – Mean parameter values, model fit and standard deviations after optimization with the averaged data configuration for each subject, over all trials.

Parameter	Subject 7	SD	Subject 8	SD	Subject 9	SD	Subj. 10	SD	Subj. 11	SD	Subj. 12	SD
m	1.765	0.979	1.710	0.883	2.216	0.496	1.773	0.849	2.261	0.626	1.200	0.000
k_{tri}	189.184	45.568	205.888	53.699	203.474	49.769	175.838	19.762	191.419	62.109	247.702	21.399
k_{tib}	230.823	211.794	114.256	19.736	103.986	3.694	102.098	3.633	153.113	81.375	110.243	17.741
$x_{0,tri}$	0.012	0.002	0.014	0.004	0.016	0.005	0.011	0.001	0.013	0.006	0.022	0.002
$x_{0,tib}$	0.060	0.027	0.054	0.010	0.045	0.004	0.048	0.001	0.059	0.018	0.058	0.005
τ_{rel}	1.418	1.328	2.235	1.517	4.232	1.485	4.852	1.989	3.006	0.945	4.263	3.009
k_{rel}	0.375	0.137	0.614	0.435	0.708	0.498	0.335	0.240	0.407	0.276	0.235	0.025
$g_1(TA)$	7.50E+04	7.57E+04	1.06E+05	9.31E+04	7.77E+04	6.65E+04	6.25E+04	5.33E+04	1.54E+05	2.65E+05	1.93E+05	6.28E+04
$g_2(GL)$	4.73E+04	6.94E+04	8.16E+04	7.07E+04	2.42E+05	2.31E+05	9.89E+01	1.70E+02	5.76E+05	9.53E+05	3.81E+05	5.99E+04
$g_3(SO)$	4.58E+04	4.45E+04	3.75E+04	3.06E+04	1.96E+05	1.73E+05	9.97E+03	9.91E+03	8.41E+04	1.20E+05	3.06E+05	5.30E+05
$g_4(GM)$	8.38E+04	8.13E+04	7.78E+04	6.67E+04	3.15E+04	5.45E+04	2.18E+05	1.87E+05	1.47E+05	2.53E+05	1.44E+05	3.03E+04
$l_{0,tri}$	0.043	0.004	0.040	0.004	0.048	0.004	0.048	0.004	0.049	0.008	0.051	0.009
$l_{0,tib}$	0.081	0.031	0.094	0.025	0.084	0.017	0.088	0.018	0.064	0.023	0.103	0.012
f_0	1.944	0.052	2.517	0.452	2.212	0.205	2.515	0.456	1.958	0.045	1.658	1.038
β	0.817	0.184	0.888	0.180	0.900	0.129	1.004	0.100	1.084	0.129	0.974	0.251
RMSE	1.366	0.901	1.108	0.553	1.254	0.550	1.135	0.099	1.227	0.652	0.738	0.373
VAF	93.177	8.899	94.291	4.704	94.994	5.339	97.349	1.364	90.997	6.877	98.806	0.599

Table 17.1 – Mean parameter values, model fit and standard deviations after optimization with the simplified model configuration for each subject, over all trials.

Parameter	Subject 1	SD	Subject 2	SD	Subject 3	SD	Subject 4	SD	Subject 5	SD	Subject 6	SD
m	1.326	0.649	1.744	0.712	1.564	0.679	2.803	0.390	1.200	0.000	1.221	0.088
k_{tri}	225.518	82.152	255.800	49.449	266.287	57.773	209.212	42.858	307.659	35.482	249.130	57.121
k_{tib}	117.000	50.604	169.227	98.076	108.351	15.884	426.059	122.473	130.055	44.104	145.416	73.374
$x_{0,tri}$	0.014	0.006	0.015	0.004	0.015	0.003	0.014	0.006	0.021	0.002	0.016	0.005
$x_{0,tib}$	0.045	0.019	0.063	0.015	0.042	0.010	0.080	0.008	0.046	0.020	0.048	0.021
τ_{rel}	1.947	1.503	2.221	1.910	2.915	2.287	1.285	1.108	0.629	0.383	1.295	1.265
k_{rel}	0.744	0.383	0.640	0.335	0.612	0.318	0.375	0.238	0.951	0.207	0.766	0.346
$g_1(TA)$	9.94E+02	2.86E+03	1.53E+02	4.77E+02	2.02E+04	5.85E+04	3.17E+04	7.54E+04	2.51E+02	1.23E+02	1.07E+04	3.66E+04
$g_2(GL)$	8.67E+04	1.65E+05	1.16E+05	2.66E+05	9.50E+04	2.34E+05	9.64E+04	2.10E+05	1.18E+03	1.29E+03	3.58E+04	8.76E+04
$g_3(SO)$	1.62E+04	6.49E+04	2.18E+04	2.97E+04	6.44E+04	1.59E+05	8.67E+04	1.69E+05	2.52E+03	4.53E+03	1.14E+04	2.03E+04
$g_4(GM)$	7.29E+03	2.51E+04	1.00E+04	2.07E+04	1.01E+04	2.66E+04	3.22E+04	1.15E+05	1.50E+02	4.16E+02	1.86E+04	2.96E+04
f_0	1.206	0.576	1.514	0.527	1.772	0.828	1.414	0.798	2.449	1.278	1.281	0.654
β	1.036	0.333	0.935	0.213	1.208	0.080	1.134	0.185	1.187	0.167	1.250	0.000
RMSE	2.191	1.138	1.097	0.464	2.316	0.966	1.475	0.841	2.511	1.623	2.717	1.892
VAF	87.563	9.041	96.854	2.096	90.870	4.950	96.963	2.093	86.465	9.854	85.705	11.470

Table 17.2 – Mean parameter values, model fit and standard deviations after optimization with the simplified model configuration for each subject, over all trials.

Parameter	Subject 7	SD	Subject 8	SD	Subject 9	SD	Subj. 10	SD	Subj. 11	SD	Subj. 12	SD
m	1.203	0.014	1.200	0.000	1.286	0.365	1.200	0.000	1.547	0.619	1.200	0.000
k_{tri}	327.292	76.268	324.908	84.511	278.520	64.439	279.855	52.838	256.023	47.253	304.402	56.264
k_{tib}	146.946	76.588	128.265	41.593	127.108	47.205	120.867	30.744	143.479	85.338	104.635	7.098
$x_{0,tri}$	0.022	0.005	0.023	0.004	0.019	0.005	0.021	0.003	0.018	0.004	0.023	0.003
$x_{0,tib}$	0.048	0.021	0.053	0.015	0.047	0.017	0.048	0.015	0.054	0.015	0.043	0.009
τ_{rel}	0.964	1.302	1.663	1.955	1.283	1.832	2.414	2.382	2.749	1.977	0.590	0.215
k_{rel}	0.654	0.369	0.738	0.385	0.828	0.299	0.419	0.352	0.718	0.352	0.795	0.307
$g_1(TA)$	9.99E+03	4.08E+04	1.46E+05	2.49E+05	5.40E+04	1.60E+05	1.35E+05	2.02E+05	3.29E+04	9.32E+04	2.21E+02	2.67E+02
$g_2(GL)$	5.01E+03	1.07E+04	8.21E+04	1.43E+05	2.75E+04	6.95E+04	1.02E+05	1.82E+05	5.34E+04	1.27E+05	1.78E+03	2.67E+03
$g_3(SO)$	7.34E+04	2.80E+05	1.93E+04	5.32E+04	5.96E+02	1.49E+03	7.66E+04	1.58E+05	1.98E+04	3.66E+04	1.35E+03	2.35E+03
$g_4(GM)$	2.60E+04	7.34E+04	6.88E+04	1.47E+05	9.52E+03	2.51E+04	7.01E+04	1.38E+05	6.35E+04	1.40E+05	8.35E+02	1.47E+03
f_0	1.314	0.638	1.513	0.859	1.807	0.920	1.758	0.903	1.406	0.631	1.555	1.154
β	0.991	0.264	1.074	0.281	1.098	0.245	1.201	0.113	1.078	0.240	0.926	0.338
RMSE	1.594	0.863	1.422	0.813	1.644	0.881	2.597	1.740	0.761	0.293	2.228	1.451
VAF	92.580	4.991	88.334	8.947	92.190	6.351	87.644	9.492	96.382	2.132	87.809	8.808

Table 18.1 – Mean parameter values, model fit and standard deviations after optimization with the model configuration containing the EMG offset subtraction parameter, for each subject, over all trials.

Parameter	Subject 1	SD	Subject 2	SD	Subject 3	SD	Subject 4	SD	Subject 5	SD	Subject 6	SD
m	1.615	0.622	1.653	0.613	1.666	0.632	2.803	0.464	1.365	0.479	1.585	0.602
k_{tri}	229.828	96.971	250.987	38.226	250.145	59.607	192.201	28.485	240.414	32.796	224.421	53.651
k_{tib}	114.121	34.038	163.917	97.069	136.780	116.579	322.391	179.024	121.016	39.293	128.135	56.744
$x_{0,tri}$	0.014	0.005	0.015	0.003	0.014	0.004	0.012	0.004	0.017	0.003	0.014	0.005
$x_{0,tib}$	0.046	0.013	0.061	0.017	0.046	0.015	0.080	0.013	0.050	0.014	0.047	0.016
τ_{rel}	2.194	1.236	2.097	1.641	2.336	1.881	1.609	1.119	2.044	1.615	1.301	0.669
k_{rel}	0.700	0.392	0.620	0.334	0.530	0.310	0.304	0.263	0.470	0.329	0.736	0.385
$g_1(TA)$	5.17E+03	1.93E+04	4.40E+03	1.35E+04	1.76E+05	5.45E+05	7.48E+05	2.65E+06	1.27E+03	5.08E+02	2.81E+05	7.71E+05
$g_2(GL)$	3.15E+04	5.31E+04	9.95E+04	2.27E+05	1.39E+05	4.31E+05	3.83E+04	9.45E+04	1.19E+04	1.23E+04	3.75E+04	4.87E+04
$g_3(SO)$	1.69E+04	5.89E+04	4.40E+04	7.59E+04	1.12E+05	2.75E+05	5.83E+04	9.15E+04	5.81E+04	5.15E+04	1.11E+04	2.33E+04
$g_4(GM)$	4.89E+03	1.07E+04	4.69E+04	1.86E+05	1.86E+04	2.95E+04	1.73E+04	6.95E+04	7.14E+03	8.56E+03	2.44E+04	4.40E+04
$l_{0,tri}$	0.057	0.015	0.042	0.010	0.051	0.016	0.049	0.012	0.080	0.016	0.054	0.018
$l_{0,tib}$	0.073	0.040	0.059	0.039	0.074	0.038	0.070	0.030	0.110	0.000	0.082	0.021
f_0	1.738	0.765	1.345	0.468	1.715	0.666	1.517	0.723	2.058	0.463	1.377	0.602
β	1.090	0.198	1.001	0.231	1.203	0.071	1.090	0.200	1.155	0.207	1.215	0.080
$B_1(TA)$	0.214	0.303	0.255	0.302	0.089	0.159	0.387	0.492	0.001	0.002	0.166	0.379
$B_2(GL)$	0.304	0.458	0.174	0.357	0.335	0.484	0.003	0.015	0.660	0.481	0.463	0.500
$B_3(SO)$	0.308	0.451	0.176	0.381	0.335	0.484	0.003	0.015	0.667	0.485	0.462	0.498
$B_4(GM)$	0.309	0.452	0.173	0.358	0.335	0.484	0.004	0.016	0.676	0.473	0.464	0.500
RMSE	2.280	1.259	1.073	0.475	2.297	1.540	1.747	1.135	1.922	0.926	2.534	1.681
VAF	87.198	10.673	96.975	1.962	90.163	10.917	95.523	4.053	92.103	5.055	87.858	9.392

Table 18.2 – Mean parameter values, model fit and standard deviations after optimization with the model configuration containing the EMG offset subtraction parameter, for each subject, over all trials.

Parameter	Subject 7	SD	Subject 8	SD	Subject 9	SD	Subj. 10	SD	Subj. 11	SD	Subj. 12	SD
m	1.244	0.129	1.268	0.289	1.329	0.390	1.319	0.337	1.625	0.603	1.253	0.219
k_{tri}	282.313	37.047	276.808	63.305	243.804	45.340	263.783	79.525	248.816	51.940	269.729	71.941
k_{tib}	163.306	86.116	164.190	117.899	140.315	73.939	149.101	90.097	132.694	63.462	104.918	7.171
$x_{0,tri}$	0.020	0.003	0.020	0.005	0.018	0.005	0.019	0.006	0.017	0.004	0.021	0.005
$x_{0,tib}$	0.052	0.022	0.055	0.020	0.050	0.019	0.051	0.020	0.053	0.014	0.048	0.007
τ_{rel}	1.120	1.266	1.378	0.831	2.261	2.447	1.687	1.802	2.464	1.955	2.000	2.379
k_{rel}	0.611	0.366	0.636	0.356	0.750	0.292	0.595	0.366	0.702	0.340	0.392	0.359
$g_1(TA)$	8.65E+04	2.79E+05	1.69E+05	3.23E+05	1.34E+06	5.33E+06	3.37E+05	6.07E+05	1.24E+05	5.10E+05	1.41E+05	3.75E+05
$g_2(GL)$	1.41E+05	5.47E+05	2.13E+05	2.11E+05	2.17E+05	5.38E+05	2.06E+05	3.20E+05	1.01E+05	1.62E+05	6.35E+04	4.97E+04
$g_3(SO)$	3.23E+04	5.67E+04	4.22E+04	5.61E+04	8.84E+03	9.54E+03	7.30E+04	1.96E+05	9.94E+04	3.85E+05	1.18E+04	1.91E+04
$g_4(GM)$	5.48E+04	1.09E+05	1.42E+05	1.75E+05	1.30E+05	3.39E+05	1.25E+05	2.93E+05	1.23E+05	2.50E+05	8.97E+03	1.08E+04
$l_{0,tri}$	0.060	0.017	0.058	0.026	0.061	0.009	0.067	0.015	0.057	0.024	0.068	0.016
$l_{0,tib}$	0.084	0.035	0.099	0.027	0.086	0.037	0.090	0.030	0.063	0.033	0.090	0.033
f_0	1.493	0.754	1.685	0.869	1.830	0.977	1.529	0.845	1.462	0.663	2.208	0.871
β	1.028	0.211	1.113	0.228	1.170	0.192	1.127	0.206	1.062	0.253	1.111	0.262
$B_1(TA)$	0.127	0.266	0.029	0.121	0.045	0.127	0.052	0.142	0.014	0.021	0.066	0.242
$B_2(GL)$	0.833	0.383	0.556	0.511	0.466	0.500	0.562	0.512	0.429	0.481	0.941	0.243
$B_3(SO)$	0.833	0.383	0.556	0.511	0.496	0.511	0.562	0.512	0.413	0.470	0.941	0.243
$B_4(GM)$	0.833	0.383	0.555	0.511	0.479	0.501	0.562	0.512	0.354	0.464	0.941	0.243
RMSE	1.220	0.667	1.240	0.699	1.348	0.687	2.083	1.538	0.847	0.359	1.820	1.513
VAF	95.536	3.462	91.240	6.805	94.595	4.313	91.757	8.635	95.554	2.849	91.088	11.558